

CRYSTALLINE MICROPOROUS AND OPEN FRAMEWORK MATERIALS

XIANHUI BU

Chemistry Department, University of California, CA93106, USA

PINGYUN FENG

Chemistry Department, University of California, Riverside, CA92521, USA

A variety of crystalline microporous and open framework materials have been synthesized and characterized over the past 50 years. Currently, microporous materials find applications primarily as shape or size selective adsorbents, ion exchangers, and catalysts. The recent progress in the synthesis of new crystalline microporous materials with novel compositional and topological characteristics promises new and advanced applications. The development of crystalline microporous materials started with the preparation of synthetic aluminosilicate zeolites in late 1940s and in the past two decades has been extended to include a variety of other compositions such as phosphates, chalcogenides, and metal-organic frameworks. In addition to such compositional diversity, synthetic efforts have also been directed towards the control of topological features such as pore size and channel dimensionality. In particular, the expansion of the pore size beyond 10Å has been one of the most important goals in the pursuit of new crystalline microporous materials.

1 Introduction

Microporous materials are porous solids with pore size below 20Å [1,2,3,4]. Porous solids with pore size between 20 and 500Å are called mesoporous materials. Macroporous materials are solids with pore size larger than 500Å. Mesoporous and macroporous materials have undergone rapid development in the past decade and they are covered in other chapters of this book. A frequently used term in the field of microporous materials is “molecular sieves” [5] that refers to a class of porous materials that can distinguish molecules on the basis of size and shape. This chapter focuses on crystalline microporous materials with a three-dimensional framework and will not discuss amorphous microporous materials such as carbon molecular sieves. However, it should be kept in mind that some amorphous microporous materials can also display shape or size selectivity and have important industrial applications such as air separation [6].

The development of crystalline microporous materials started in late 1940s with the synthesis of synthetic zeolites by Barrer, Milton, Breck and their coworkers [7,8]. Some commercially important microporous materials such as zeolites A, X, and Y were made in the first several years of Milton and Breck’s work. In the following thirty years, zeolites with various topologies and chemical compositions (e.g., Si/Al ratios) were prepared, culminating with the synthesis of ZSM-5 [9] and

aluminum-free pure silica polymorph silicalite [10] in 1970s. A breakthrough leading to an extension of crystalline microporous materials to non-aluminosilicates occurred in 1982 when Flanigen *et al.* reported the synthesis of aluminophosphate molecular sieves [11,12]. This breakthrough was followed by the development of substituted aluminophosphates. Since late 1980s and the early 1990s, crystalline microporous materials have been made in many other compositions including chalcogenides and metal-organic frameworks [13,14].

Crystalline microporous materials usually consist of a rigid three-dimensional framework with hydrated inorganic cations or organic molecules located in the cages or cavities of the inorganic or hybrid inorganic-organic host framework. Organic guest molecules can be protonated amines, quaternary ammonium cations, or neutral solvent molecules. Dehydration (or desolvation) and calcination of organic molecules are two methods frequently used to remove extra-framework species and generate microporosity.

Crystalline microporous materials generally have a narrow pore size distribution. This makes it possible for a microporous material to selectively allow some molecules to enter its pores and reject some other molecules that are either too large or have a shape that does not match with the shape of the pore. A number of applications involving microporous materials utilize such size and shape selectivity.

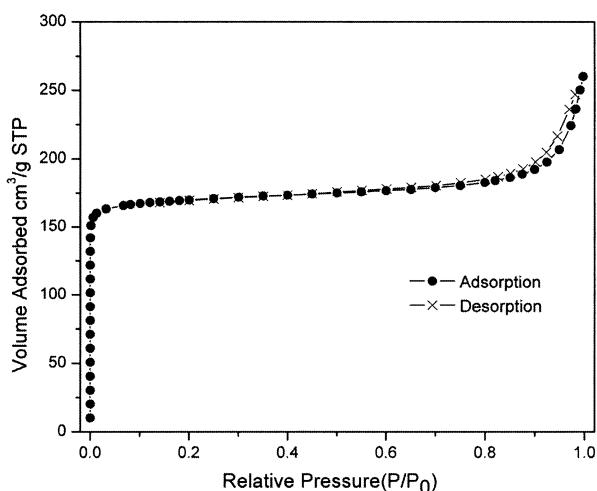


Figure 1. Nitrogen adsorption and desorption isotherms typical of a microporous material. Data were measured at 77K on a Micromeritics ASAP 2010 Micropore Analyzer for Molecular Sieve 13X. The structure of 13X is shown in Fig. 3. The sample was supplied by Micromeritics.

Two important properties of microporous materials are ion exchange and gas sorption. The ion exchange is the exchange of ions held in the cavity of microporous materials with ions in the external solutions. The gas sorption is the ability of a

microporous material to reversibly take in molecules into its void volume (Fig. 1). For a material to be called microporous, it is generally necessary to demonstrate the gas sorption property.

The report by Davis *et al.* of a hydrated aluminophosphate VPI-5 with pore size larger than 10Å in 1988 generated great enthusiasm toward the synthesis of extra-large pore materials [15]. The expansion of the pore size is an important goal of the current research on microporous materials [16]. Even though microporous materials include those with pore sizes between 10 to 20Å, The vast majority of known crystalline microporous materials have a pore size <10Å. The synthesis of microporous materials with pore size between 10 and 20Å is desirable for applications involving molecules in such size regime and remains a significant synthetic challenge today.

In the following sections, we will first review oxide-based microporous materials followed by a review on related chalcogenides. We will then discuss metal-organic frameworks, in which the framework is a hybrid between inorganic and organic units. The research on metal-organic frameworks is a rapidly developing area. These metal-organic materials are being studied not only for their porosity, but also for other properties such as chirality and non-linear optical activity [17]. The last section gives a discussion on materials with extra-large pore sizes. There exist many excellent reviews and books from which readers can find detailed information on various zeolite and phosphate topics [1,4,13,18,19,20,21,22,23,24,25].

2 Microporous Silicates

From a commercial perspective, the most important microporous materials are zeolites, a special class of microporous silicates. A strict definition of zeolites is difficult [5] because both chemical compositions and geometric features are involved. Zeolites can be loosely considered as crystalline three-dimensional aluminosilicates with open channels or cages. Not all zeolites are microporous because some are unable to retain their framework once extra-framework species (e.g., water or organic molecules) are removed. The stability of zeolites varies greatly depending on framework topologies and chemical compositions such as the Si/Al ratio and the type of charge-balancing cations. In addition to aluminum, many other metals have been found to form microporous silicates such as gallosilicates [26], titanosilicates [27,28], and zincosilicates [16]. Some microporous frameworks can even be made as pure silica polymorphs, SiO₂ [10].

2.1 Chemical compositions and framework structures of zeolites

Natural zeolites are crystalline hydrated aluminosilicates of group IA and group IIA elements such as Na⁺, K⁺, Mg²⁺, and Ca²⁺. Chemically, they are represented by the empirical formula: M_{2n}O•Al₂O₃•ySiO₂ •wH₂O where y is 2 or larger, n is the cation

valence, and w represents the water contained in the voids of the zeolite. An empirical rule, Loewenstein rule [29], suggests that in zeolites, only Si-O-Si and Si-O-Al linkages be allowed. In other words, the Al-O-Al linkage does not occur in zeolites and the Si/Al molar ratio is ≥ 1 .

Synthetic zeolites fall into two families on the basis of extra-framework species. One family is similar to natural zeolites in chemical compositions. These zeolites have a low Si/Al ratio that is usually less than 5. The other family of zeolites are made with organic structure-directing agents and they generally have a Si/Al ratio larger than 5.

In the absence of the framework interruption, the overall framework formula of a zeolite is AO_2 just like SiO_2 . When A is Si^{4+} , no framework charge is produced. However, for each Al^{3+} , a negative charge develops on the framework. The negative charge is balanced by either inorganic or organic cations located in channels or cages of the framework. The charge-balancing cations are usually mobile and can undergo ion exchange.

Frameworks of zeolites are based on the three-dimensional, four-connected network of AlO_4 and SiO_4 tetrahedra linked together through the corner-sharing of oxygen anions. In a zeolite framework, oxygen atoms are bi-coordinated between two tetrahedral cations. When describing a zeolite framework, oxygen atoms are often omitted and only the connectivity among tetrahedral atoms is taken into consideration (Fig. 2).

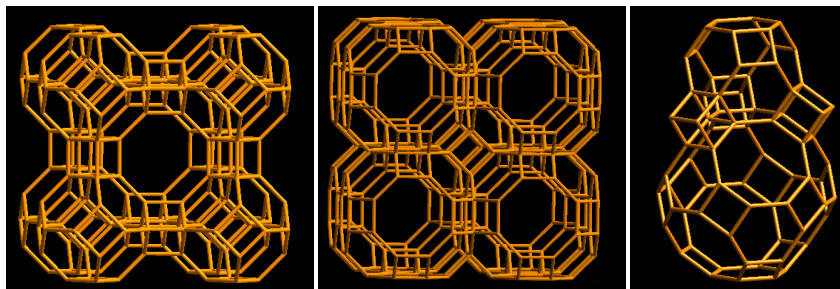


Figure 2. The three-dimensional framework of small-pore zeolite A (LTA) showing connectivity among framework tetrahedral atoms. (Left) viewed as sodalite cages linked together through double 4-rings (D4R); (middle) viewed as α -cages linked together by sharing single 8-rings; (right) three different cage units in zeolite A. The cage on top is called the β (or sodalite) cage and is built from 24 tetrahedral atoms. The cage at bottom is called the α cage and has 48 tetrahedral atoms. Also shown are three D4R's. Reprinted with permission from <http://www.iza-structures.org/> and reference [30].

Zeolites and zeolite-like oxides are classified according to their framework types. A framework type is determined based on the connectivity of tetrahedral atoms and is independent of chemical compositions, types of extra-framework species, crystal symmetry, unit cell dimensions, or any other chemical and physical properties. In theory, there are numerous ways to connect tetrahedral atoms into a

three-dimensional, four-connected network. However, in practice, only a very limited number of topological types have been found. In the past two decades, new framework topologies have been found mainly in non-zeolites such as open framework phosphates.

Even taking into consideration of both zeolites and non-zeolites, synthetic and natural solids, there are only 133 framework types listed in the “Atlas of Zeolite Framework Types” published by the structure commission of the International Zeolite Association [30]. These framework types are also published on the internet at <http://www.iza-structures.org/>. Each framework type in the ATLAS is assigned a three capital letter code. For example, FAU designates the framework type of a whole family of materials (e.g., SAPO-37, [Co-Al-P-O]-FAU, zeolites X and Y) with the same topology as the mineral faujasite (Fig. 3) [30]. Those codes help to clear the confusion resulting from many different names given to materials with different chemical compositions, but with the same topology. Sometimes even the same material can have different names assigned by different laboratories.

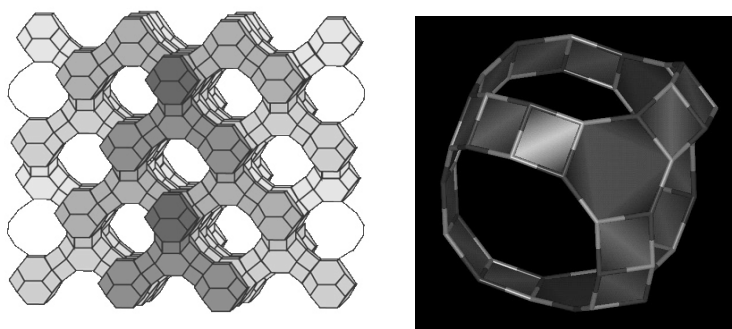


Figure 3. (left) The three-dimensional framework of the mineral faujasite (FAU). Zeolites X and Y have the same topology as faujasite, but zeolite Y has a higher Si/Al ratio than zeolite X. Reprinted with permission from <http://www.iza-structures.org/> and reference [30]. (right) The faujasite supercage with 48 tetrahedral atoms. The cage can be assembled from four 6-rings and six 4-rings. Four 12-ring windows are arranged tetrahedrally.

An important structural parameter is the size of the pore opening through which molecules diffuse into channels and cages of a zeolite. The pore size is related to the ring size defined as the number of tetrahedral atoms forming the pore. In the literature, zeolites with 8-ring, 10-ring, and 12-ring windows are often called small-pore, medium-pore, and large-pore zeolites, respectively. In addition to the ring size, the pore size is affected by other factors such as the ring shape, the size of tetrahedral atoms, the type of non-framework cations. For example, molecular sieves 3A, 4A, and 5A all have the same zeolite A (LTA) structure and the difference in the pore size is caused by different extra-framework cations (K^+ , Na^+ , and Ca^{2+} , respectively).

The pore volume of a zeolite is related to the framework density defined as the number of tetrahedral atoms per 1000\AA^3 . For zeolites, the observed values range from 12.7 for faujasite to 20.6 for cesium aluminosilicate (CAS) [30]. In general, the framework density does not reflect the size of the pore openings. For example, CIT-5 has an extra-large pore size with 14-ring windows, but its framework density is 18.3, significantly larger than that of faujasite (12.7) with 12-ring windows [30]. In general, large pore sizes, large cages, and multidimensional channel systems are three important factors that contribute to a low framework density for a four-connected, three-dimensional framework.

The framework density has been increasingly used to describe non-zeolites. The care must be taken when comparing the framework density of two compounds because the framework density can be significantly altered by framework interruptions (e.g., terminal OH groups) that can lead to a substantial decrease in the framework density. Even for the same framework topology, a change in the chemical composition will lead to a change in bond distances and consequently in unit cell volumes. This will result in either an increase or decrease in the framework density.

All zeolites are built from TO_4 tetrahedra, called primary (or basic) building units. Larger finite units with three to sixteen tetrahedra (called Secondary Building Units or SBU's) are often used to describe the zeolite framework [30]. A SBU is a finite structural unit that can alone or in combination with another one build up the whole framework. The smallest SBU is a 3-ring, but it rarely occurs in zeolite framework types. Instead, 4-rings and 6-rings are most common in zeolite and zeolite-like structures.

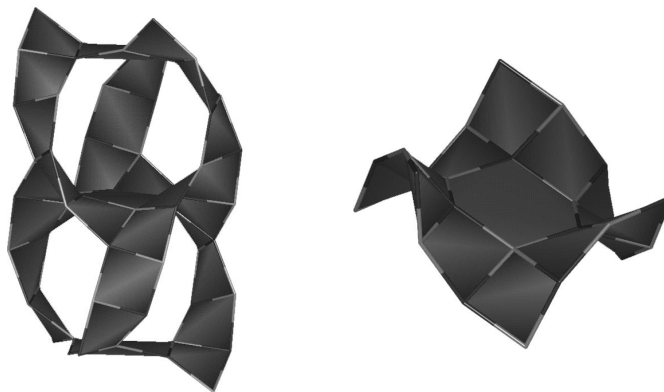


Figure 4. The wall structure of UCSB-7. UCSB-7 is one of a number of zeolite or zeolite-like structures that can be described using a minimal surface. UCSB-7 can be readily synthesized as germanate or arsenate, but has not been found as silicate or phosphate.

There are several other ways to describe the framework topology of a zeolite. For example, structural units larger than SBU's can be used. In this way, zeolites

can be described as packing of small cages or clusters, cross-linking of chains, and stacking of layers with various sequences [31]. Some zeolite and zeolite-like frameworks can also be described using minimal surfaces (Fig. 4) [32].

When zeolite structures are described using clusters or cage units, these clusters and cages can be considered as large artificial atoms. Under such circumstances, structures of zeolites can be simplified to some of the simplest structures such as diamond and metals (e.g., fcc, ccp, and bcp). For examples, zeolite A is built from the simple cubic packing of sodalite cages and zeolite X has the diamond-type structure with the center of the sodalite cages occupying the tetrahedral carbon sites in diamond. Because these artificial atoms (clusters or cages) often have lower symmetry than a real spherical atom, the overall crystal symmetry can be lower than the parent compounds.

2.2 High silica or pure silica molecular sieves

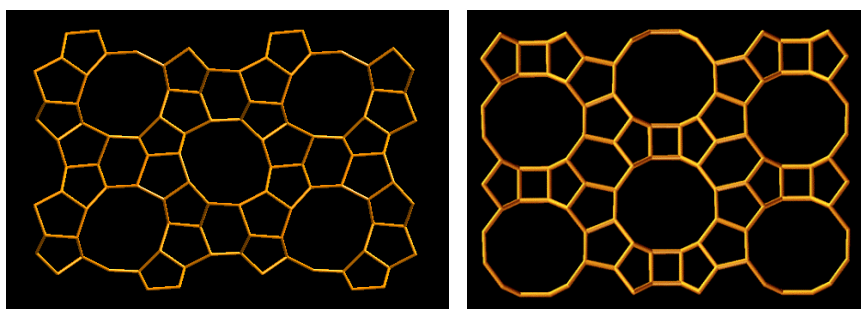


Figure 5. (Left) The framework of ZSM-5 projected down the [010] direction showing the 10-ring straight channels. ZSM-5 is thus far the most important crystalline microporous material discovered by using the organic structure-directing agent. It also has a large number of 5-rings that are common in high silica zeolites. (right) the framework of zeolite beta (polymorph A) projected down the [100] direction. Zeolite beta is an important zeolite because its framework is chiral and because it has a three-dimensional 12-ring channel system. Reprinted with permission from <http://www.iza-structures.org/> and reference [30].

In the past three decades, synthetic efforts directly related to aluminosilicate zeolites are generally in the area of high silica ($\text{Si/Al} > 5$) or pure silica molecular sieves [33]. The use of organic bases has had a significant impact on the development of high silica zeolites. The Si/Al ratio in the framework is increased because of the low charge to volume ratios of organic molecules. In general, the crystallization temperature (about 100-200°C) is higher than that required for the synthesis of hydrated zeolites. Alkali-metal ions, in addition to the organic materials, are usually used to help control the pH and promote the crystallization of high silica zeolites.

One of the most important zeolites created by this approach is ZSM-5 (Fig. 5), originally prepared using tetrapropylammonium cations as the structure-directing agent [9]. ZSM-5 (MFI) has a high catalytic activity and selectivity for various reactions. The pure silica form of ZSM-5 is called silicalite [10]. Another important zeolite is zeolite beta shown in Figure 5.

The use of fluoride media has been found to generate some new phases [34]. Frequently, crystals prepared from the fluoride medium have better quality and larger size compared to those made from the hydroxide medium [35]. In addition to serve as the mineralizing agent, F⁻ anions can also be occluded in the cavities or attached to the framework cations. This helps to balance the positive charge of organic cations. Upon calcination of high silica or pure silica phases, F⁻ anions are usually removed together with organic cations.

Among recently created high silica or pure silica molecular sieves are a series of materials denoted as ITQ-*n* synthesized from the fluoride medium. By employing H₂O/SiO₂ ratios lower than those typically used in the synthesis of zeolites in F⁻ or OH⁻ medium, a series of low-density silica phases were prepared [36]. Some of these (i.e., ITQ-3, ITQ-4, and ITQ-7) possess framework topologies not previously known in either natural or synthetic zeolites [37,38,39]. Another structure with a novel topology is germanium-containing ITQ-21 [40]. Similar to faujasite, ITQ-21 is also a large pore and large cage molecular sieve with a three-dimensional channel system. However, the cage in ITQ-21 is accessible through six 12-ring windows compared to four in faujasite.

The double 4-ring unit (D4R) as found in zeolite A often leads to a highly open architecture. However, for the aluminosilicate composition, it is a strained unit and does not occur often. The synthesis of ITQ-21 is related to the synthetic strategy that the incorporation of germanium helps stabilize the D4R. Similarly, during the synthesis of ITQ-7, the incorporation of germanium substantially reduced the crystallization time from 7 days to 12 hours [41]. The use of germanium has also led to the synthesis of the pure polymorph C of zeolite beta (BEC) even in the absence of the fluoride medium that is generally believed to assist in the formation of D4R units [42]. Both ITQ-7 and the polymorph C of zeolite beta contain D4R units and their syntheses were strongly affected by the presence of germanium.

The effect of germanium in the synthesis of D4R-containing high silica molecular sieves reflects a more general observation that there is a correlation between the framework composition and the preferred framework topology. For example, UCSB-7 can be easily synthesized in germanate or arsenate compositions [32], but has never been made in the silicate composition.

In general, large T-O distances and small T-O-T angles tend to favor more strained SBU's such as 3-rings and D4R units. It has already been observed that the germanate composition favors 3-rings and D4R units [43,44]. This observation can be extended to non-oxide open framework materials such as halides (e.g., CZX-2) [45], sulfides, and selenides with four-connected, three-dimensional topologies [46].

In these compositions, the T-X-T (X = Cl, S, and Se) angles are around 109° and three-rings become common. The presence of 3-rings is desirable because it could lead to highly open frameworks [30].

2.3 Low and intermediate silica molecular sieves

Low ($\text{Si}/\text{Al} \leq 2$) and intermediate ($2 < \text{Si}/\text{Al} \leq 5$) silica zeolites [18] are used as ion exchangers and have also found use as adsorbents for applications such as air separation. Syntheses of low and intermediate zeolites are usually performed under hydrothermal conditions using reactive alkali-metal aluminosilicate gels at low temperatures (~100°C and autogenous pressures). The synthesis procedure involves combining alkali hydroxide, reactive forms of alumina and silica, and H₂O to form a gel. Crystallization of the gel to the zeolite phase occurs at a temperature near 100°C. Two most important zeolites prepared by this approach are zeolites A and X [47]. The framework topology of zeolite A has not been found in nature. Zeolite X is compositionally different but topologically the same as mineral faujasite. Both zeolite A and zeolite X are built from packing of sodalite cages. In zeolite A, sodalite cages are joined together through 4-rings (Fig. 2) whereas in zeolite X, sodalite cages are coupled through 6-rings (Fig. 3).

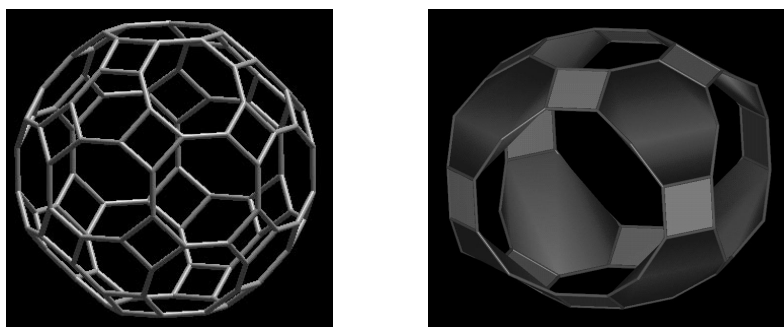


Figure 6. (left) The tschortnerite cage built from 96 tetrahedral atoms. Reprinted with permission from <http://www.iza-structures.org/> and reference [30]. (right) The UCSB-8 cage built from 64 tetrahedral atoms [30].

Few synthetic low and intermediate silica zeolites with new framework types have been reported in the past three decades. However, some new topologies have been found in natural zeolites. The most interesting one is a recently discovered mineral tschortnerite [48] with a Si/Al ratio of 1. This structure consists of several well-known structural units in zeolites including double 6-rings, double 8-rings, α -cages, and β -cages. Of particular interest is the presence of a cage (tschortnerite cage) with 96 tetrahedral atoms (Fig. 6), the largest known cage in four-connected,

three-dimensional networks. In terms of the number of tetrahedral atoms, the tschortnerite cage is twice as large as the supercage in faujasite. However, the tschortnerite cage is accessible through 8-rings that are smaller than the 12-ring windows in faujasite.

The difficulty involving the creation of new low and intermediate silica molecular sieves is in part because of the limited choice in structure-directing agents. Traditionally, inorganic cations such as Na^+ are employed and it has not been possible to synthesize zeolites with a Si/Al ratio smaller than 5 with organic cations. However, recent results demonstrate that organic cations can template the formation of M^{2+} substituted alumino- (gallo-)phosphate open frameworks in which the $\text{M}^{2+}/\text{M}^{3+}$ molar ratio is ≤ 1 [49,50]. In terms of the framework charge per tetrahedral unit, this is equivalent to aluminosilicates with a Si/Al ratio ≤ 3 . Thus, it might be feasible to prepare low and intermediate silica zeolites using amines as structure-directing agents.

3 Microporous and Open Framework Phosphates

Because of the structural similarity between dense SiO_2 and AlPO_4 phases, the research in the 1970s on high silica or pure silica molecular sieves quickly led to the realization that it might be possible to synthesize aluminophosphate molecular sieves using the method similar to that employed for the synthesis of silicalite. In 1982, Flanigen *et al.* reported a major discovery of a new class of aluminophosphate molecular sieves ($\text{AlPO}_4\text{-n}$) [11,12]. Unlike zeolites that are capable of various Si/Al ratios, the framework of these aluminophosphates consists of alternating Al^{3+} and P^{5+} sites and the overall framework is neutral with a general formula of AlPO_4 .

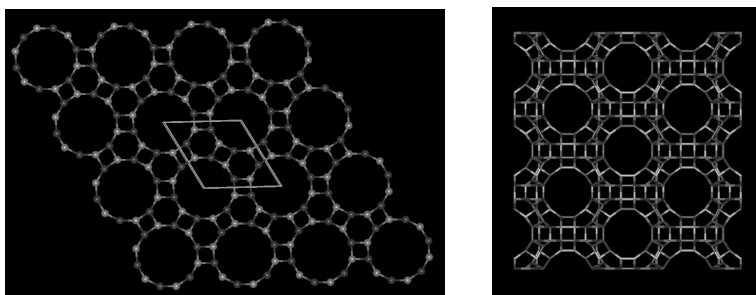


Figure 7. (Left) The three-dimensional framework of $\text{AlPO}_4\text{-5}$ consists of one-dimensional 12-ring channels. Note the alternating distribution of P and Al sites. Red: P, Yellow: Al. (right) 12-ring channels in metal (Co, Mn, Mg) substituted aluminophosphate UCSB-8.

These aluminophosphates are synthesized hydrothermally using organic amines or quaternary ammonium salts as structure-directing agents. In most cases, organic molecules are occluded into the channels or cages of AlPO_4 frameworks. Because

the framework is neutral, the positive charge of organic cations is balanced by the simultaneous occlusion of OH⁻ groups. Many of these aluminophosphates have a high thermal stability and remain crystalline after calcination at temperatures between 400-600°C. In addition to framework types already known in zeolites, new topologies have also been found in some structures including AlPO₄-5 (AFI) that has a one-dimensional 12-ring channel (Fig. 7) [51].

The next family of new molecular sieves consists of a series of silicon substituted aluminophosphates [52] called silicoaluminophosphates (SAPO-n). To avoid the Si-O-P linkage, Si⁴⁺ cations tend to replace P⁵⁺ sites or both Al³⁺ and P⁵⁺ sites. The substitution of P⁵⁺ sites by Si⁴⁺ cations produces negatively charged frameworks with cation exchange properties and acidic properties. The SAPO family includes two new framework types, SAPO-40 (AFR) and SAPO-56 (AFX), not previously known in aluminosilicates, pure silica polymorphs, or aluminophosphates [30].

In addition to silicon, other elements can also be incorporated into aluminophosphates. In 1989, Wilson and Flanigen [53] reported a large family of metal aluminophosphate molecular sieves (MeAPO-n). The metal (Me) species include divalent forms of Mg, Mn, Fe, Co, and Zn (M²⁺). The MeAPO family represents the first demonstrated synthesis of divalent metal cations in microporous frameworks [53]. In one of these phases, CoAPO-50 (AFY) with a formula of [(C₃H₇)₂NH₂]₃[Co₃Al₅P₈O₃₂]•7H₂O, approximately 37% of Al³⁺ sites are replaced with Co²⁺ cations [30]. For each substitution of Al³⁺ by M²⁺, a negative charge develops on the framework, which is balanced by protonated amines or quaternary ammonium cations.

For a given framework topology, the framework charge is tunable in aluminosilicates by changing Si/Al ratios. However, it is fixed in binary phosphates such as aluminophosphates or cobalt phosphates [30,54]. The use of ternary compositions as in metal aluminophosphates provides the flexibility in adjusting the framework charge density. Such flexibility contributes to the development of a large variety of new framework types in metal aluminophosphates and has also led to the synthesis of a large number of phosphates with the same framework type as those in zeolites [30,50].

The MeAPSO family further extends the structural diversity and compositional variation found in the SAPO and MeAPO molecular sieves. MeAPSO can be considered as double (Si⁴⁺ and M²⁺) substituted aluminophosphates. The MeAPSO family includes one new large pore structure MeAPSO-46 with a formula of [(C₃H₇)₂NH₂]₈[Mg₆Al₂₂P₂₆Si₂O₁₁₂]•14H₂O [30]. The quaternary (four different tetrahedral elements at non-trace levels) composition is rare in a microporous framework, but is obviously a promising area for future exploration.

In the two decades following Wilson and Flanigen's original discovery, there has been an explosive growth in the synthesis of open framework phosphates [13,55]. It is apparent that the MeAPO's exhibit much more structural diversity and

compositional variation than both SAPO's and MeAPSO's. However, the thermal stability of MeAPO's is generally lower than that of either AlPO_4 's or SAPO's. In general, the thermal stability of a metal aluminophosphate decreases with an increase in the concentration of divalent metal cations in the framework.

In addition to the continual exploration of AlPO_4 and MeAPO compositions, many other compositions have been investigated including gallophosphates and metal gallophosphates [13]. Of particular interest is the synthesis of a family of extra-large pore phosphates with ring sizes larger than 12 tetrahedral atoms [16]. The use of the fluoride medium [34] and non-aqueous solvents [56] further enriches the structural and compositional diversity of the phosphate-based molecular sieves.

Unlike aluminophosphate molecular sieves developed by Flanigen *et al.*, new generations of phosphates such as phosphates of tin, molybdenum, vanadium [57], iron, titanium, and nickel often consist of metal cations with different coordination numbers ranging from three to six [13]. The variable coordination number helps the generation of many new metal phosphates.

In terms of the framework charge, AlPO_4 's, SAPO's, and MeAPO's closely resemble high silica and pure silica molecular sieves. This is not surprising because the synthetic breakthrough in aluminophosphate molecular sieves was based on the earlier synthetic successes in high silica and pure silica phases. However, for certain applications such as N_2 selective adsorbents for air separation, it is desirable to prepare aluminophosphate-based materials that are similar to low or intermediate zeolites. Because each $(\text{AlSi}_3\text{O}_8)^-$ unit carries the same charge as $(\text{MAlP}_2\text{O}_8)^-$ (M is a divalent metal cation), the M^{2+}/Al ratio of 1 is equivalent to the Si/Al ratio of 3 in terms of the framework charge per tetrahedral atom. For a Si/Al ratio of 5 as in $(\text{AlSi}_5\text{O}_{12})^-$, the corresponding M^{2+}/Al ratio is 0.5 as in $(\text{CoAl}_2\text{P}_3\text{O}_{12})^-$. Therefore, to make highly charged aluminophosphates similar to low and intermediate silica, the M^{2+}/Al ratio should be higher than 0.5. Only a very small number of compounds with M^{2+}/Al ratio ≥ 0.5 were known prior to 1997 [30,58,59].

A significant advance occurred in 1997 when a family of highly charged metal aluminophosphates with a $\text{M}^{2+}/\text{M}^{3+} \geq 1$ ($\text{M}^{2+} = \text{Co}^{2+}, \text{Mn}^{2+}, \text{Mg}^{2+}, \text{Zn}^{2+}, \text{M}^{3+} = \text{Al}^{3+}, \text{Ga}^{3+}$) were reported [49,50,60]. After over two decades of extensive research on high silica, pure silica, aluminophosphates, and other open framework materials with low-charged or neutral framework, the synthesis of these highly charged metal aluminophosphates represented a noticeable reversal towards highly charged frameworks often observed in natural zeolites. The recent work on 4-connected, three-dimensional metal sulfides and selenides further increased the framework negative charge to an unprecedented level with a $\text{M}^{4+}/\text{M}^{3+}$ ratio as low as 0.2 [46].

Three families of open framework phosphates denoted as UCSB-6 (SBS), UCSB-8 (SBE) (Fig. 7), and UCSB-10 (SBT) demonstrate that zeolite-like structures with large pore, large cage, and multidimensional channel systems can be synthesized with a framework charge density much higher than currently known organic-templated silicates [49]. The $\text{M}^{2+}/\text{M}^{3+}$ ratio in these phases is equal to 1. If

these materials could be made as aluminosilicates, the Si/Al ratio would be 3. It is worth noting that until now, no zeolites templated with organic cations only have a Si/Al ratio of 3 or lower. The synthesis of UCSB-6, UCSB-8, UCSB-10, and other highly charged phosphate-based zeolite analogs shows that it might be possible to synthesize low and intermediate silica by templating with organic cations.

While UCSB-6 and UCSB-10 have framework structures similar to EMC-2 (EMT) and faujasite (FAU), respectively, UCSB-8 has an unusual large cage consisting of 64 tetrahedral atoms. Such cage is accessible through four 12-ring windows and two 8-ring windows (Fig. 6). In comparison, the supercage in FAU-type structures is built from 48 T-atoms.

4 Microporous and Open Framework Sulfides

During the development of the above oxide-based microporous materials, two new research directions appeared in late 1980s and early 1990s. One was the synthesis of open framework sulfides initiated by Bedard, Flanigen, and coworkers [61]. Another was the development of metal-organic frameworks in which inorganic metal cations or clusters are connected with organic linkers. Metal-organic frameworks have become an important family of microporous materials and they will be discussed in the next section. Open framework chalcogenides are particularly interesting because of their potential electronic and electrooptic properties, as compared to the usual insulating properties of open framework oxides.

Like in zeolites, the tetrahedral coordination is common in metal sulfides. However, structures of open framework sulfides are substantially different from zeolites. This is mainly because of the coordination geometry of bridging sulfur anions. The typical value for the T-S-T angle in metal sulfides is between 105 and 115 degrees, much smaller than the typical T-O-T angle in zeolites that usually lies between 140 and 150 degrees. In addition, the range of the T-S-T angle is also considerably smaller than that of the T-O-T angle. While the range of the T-S-T angle is approximately between 98 and 120 degrees, the T-O-T angle can extend from about 120 to 180 degrees, depending on the type of tetrahedral atoms.

As the exploratory synthesis in zeolite and zeolite-like materials has progressed from silicates and phosphates to arsenates and germanates [62,63,64], it becomes clear that from a purely geometrical view, the research on open framework sulfides, selenide, and halides continue the trend towards large T-X distances and smaller T-X-T angles (X is an anion such as O, S, and Cl). Such trend has the potential to generate zeolite-like structures with 3-rings and exceptionally large pore sizes.

The tendency for the T-S-T angle to be close to 109 degrees has a fundamental effect on the structure of open framework sulfides. In sulfides with tetrahedral metal cations, all framework elements can adopt tetrahedral coordination. As a result, clusters with structure resembling fragments of zinc blende type lattice can be formed. These clusters are now called supertetrahedral clusters (Fig. 8).

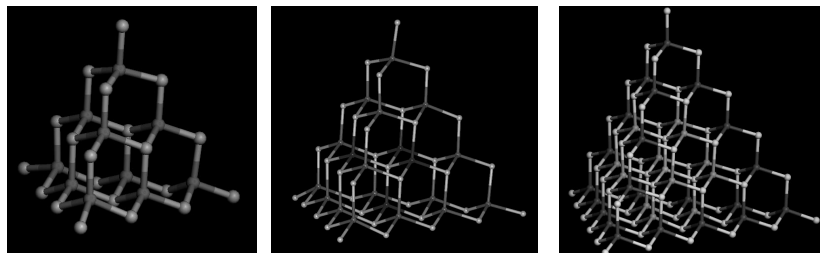


Figure 8. (left) the supertetrahedral T3 cluster, (middle) the T4 cluster. Blue sites are occupied with divalent metal cations. (right) the T5 cluster. Red: In^{3+} ; Yellow: S^{2-} ; Cyan: the core Cu^+ site. In a given cluster, only four green sites are occupied by Cu^+ ions. The occupation of green sites by Cu^+ ions is not random and follows Pauling's electrostatic valence rule.

Supertetrahedral clusters are regular tetrahedrally shaped fragments of zinc blende type lattice. They are denoted by Yaghi and O'Keeffe as T_n , where n is the number of metal layers [65,66]. One special case is T1 and it simply refers to a tetrahedral cluster such as MS_4 , where M is a metal cation. If we add an extra layer, the cluster would be shaped like an adamantane cage with the composition M_4S_{10} , called supertetrahedral T2 cluster because it consists of two metal layers. With the addition of each layer, a new supertetrahedron of a higher order will be obtained. The compositions of supertetrahedral T3, T4, and T5 clusters are $\text{M}_{10}\text{X}_{20}$ and $\text{M}_{20}\text{X}_{35}$, and $\text{M}_{35}\text{X}_{56}$ respectively. When all corners of each cluster are shared through bi-coordinated S^{2-} bridges (as in zeolites), the number of anions per cluster in the overall stoichiometry is reduced by two. While a T2 cluster consists of only bi-coordinated sulfur atoms, a T3 cluster has both bi- and tri-coordinated sulfur atoms. Starting from T4 clusters, tetrahedral coordination begins to occur for sulfur atoms inside the cluster.

At this time, the largest supertetrahedral cluster observed is the T5 cluster (Fig. 8) with the composition of $[\text{Cu}_5\text{In}_{30}\text{S}_{54}]^{13-}$ [67]. This T5 cluster occurs as part of a covalent superlattice in UCR-16 and UCR-17. So far, isolated T5 clusters have not been synthesized. The largest isolated supertetrahedral cluster known to date is T3. Some examples are $[(\text{CH}_3)_4\text{N}]_4[\text{M}_{10}\text{E}_4(\text{SPh})_{16}]$, where $M = \text{Zn}, \text{Cd}$, $E = \text{S}, \text{Se}$, and Ph is a phenyl group [68,69].

With T_n clusters as artificial tetrahedral atoms, it is possible to construct covalent superlattices with framework topologies similar to those found in zeolites. However, the ring size in terms of the number of tetrahedral atoms is increased by n times. An increase in the ring size is important because crystalline porous materials with a ring size larger than 12 are rather scarce, but highly desirable for applications involving large molecules.

4.1 Sulfides with tetravalent cations

Some zeolites such as ZSM-5 and sodalite can be made in the neutral SiO_2 form [10,56]. Neutral frameworks have also been found in microporous aluminophosphates [11] and germanates [64,70]. It is therefore reasonable to expect that microporous sulfides with a general framework composition of GeS_2 or SnS_2 may exist. The Ge-S and Sn-S systems were among the earliest compositions explored by Bedard *et al.*, when they reported their work on open framework sulfides in 1989. Thus far, a number of new compounds were found in Ge-S and Sn-S compositions, however, very few have three-dimensional framework structures. Frequently, molecular, one-dimensional, or layered structures are found in these compositions.

In the Ge-S system, the largest observed supertetrahedral cluster is T2 ($\text{Ge}_4\text{S}_{10}^{4-}$). Larger clusters such as T3 have not been found in the Ge-S system possibly because the charge on germanium is too high to satisfy the coordination environment of tri-coordinated sulfur sites that exist in clusters larger than T2. This is because of Pauling's Electrostatic Valence Rule that suggests the charge on an anion must be balanced locally by neighboring cations.

Isolated T2 clusters ($\text{Ge}_4\text{S}_{10}^{4-}$) have been found to occur [71,72,73] in the molecular compound $[(\text{CH}_3)_4\text{N}]_4\text{Ge}_4\text{S}_{10}$. One-dimensional chains of $\text{Ge}_4\text{S}_{10}^{4-}$ clusters have also been observed in a compound called DPA-GS-8 [74]. One polymorph of GeS_2 , $\delta\text{-GeS}_2$, consists of covalently linked $\text{Ge}_4\text{S}_{10}^{4-}$ clusters with a three-dimensional framework [75]. The framework topology resembles that of the diamond type lattice, however, the extra-framework space is reduced because of the presence of two interpenetrating lattices. As shown in later sections, the interpenetration can be removed by incorporating trivalent metal cations into the cluster to generate negative inorganic frameworks that can be assembled with protonated amines.

In the Sn-S system, layered structures are common [76]. Because of its large size, tin frequently forms non-tetrahedral coordination. In addition, tin may also form oxysulfides, which further complicates the synthetic design of porous tin sulfides. One rare three-dimensional framework [77] based on tin sulfide is $[\text{Sn}_5\text{S}_9\text{O}_2][\text{HN}(\text{CH}_3)_3]_2$. This material is built from T3 clusters, $[\text{Sn}_{10}\text{S}_{20}]$. Each T3 cluster has four adamantane-type cavities that can accommodate one oxygen atom per cavity to give a cluster $[\text{Sn}_{10}\text{S}_{20}\text{O}_4]^{8-}$. Because each corner sulfur atom is shared between two clusters. The overall framework formula is $[\text{Sn}_{10}\text{S}_{18}\text{O}_4]^{4-}$. The isolated form of the $[\text{Sn}_{10}\text{S}_{20}\text{O}_4]^{8-}$ cluster is also known in $\text{Cs}_8\text{Sn}_{10}\text{S}_{20}\text{O}_4 \cdot 13\text{H}_2\text{O}$ [78].

4.2 Sulfides with tetravalent and mono- or divalent cations

The early success in the preparation of open framework sulfides depended primarily on the use of mono- or divalent cations (e.g., Cu^+ , Mn^{2+}) to join together chalcogenide clusters (e.g., $\text{Ge}_4\text{S}_{10}^{4-}$). These low-charged mono- or divalent cations

help generate negative charges on the framework that are usually charge-balanced by protonated amines or quaternary ammonium cations.

One example was the synthesis of TMA-CoMnGS-2 [61]. Like many other germanium sulfides, the basic structural unit is the T2 cluster. Here, T2 clusters are joined together by three-connected $\text{Me}(\text{SH})^+$ (Me = divalent metal cations such as Co^{2+} and Mn^{2+}) units to form a framework structure. Another interesting example was the synthesis of a series of compounds with the general formula of $[(\text{CH}_3)_4\text{N}]_2\text{MGe}_4\text{S}_{10}$ (M = Mn^{2+} , Fe^{2+} , Cd^{2+}) [73,79,80]. Unlike $\delta\text{-GeS}_2$ that is an intergrowth of two diamond-type lattice (double-diamond type), $[(\text{CH}_3)_4\text{N}]_2\text{MGe}_4\text{S}_{10}$ has a non-interpenetrating diamond-type lattice (single-diamond type) in which tetrahedral carbon sites are replaced with alternating T2 and T1 clusters.

In $[(\text{CH}_3)_4\text{N}]_2\text{MGe}_4\text{S}_{10}$ and TMA-CoMnGS-2, the divalent metal cations join together four and three T2 clusters, respectively. It is also possible for a metal cation to connect to only two T2 clusters. Such is the case in $\text{CuGe}_2\text{S}_5(\text{C}_2\text{H}_5)_4\text{N}$, in which T2 clusters form the single-diamond type lattice with monovalent Cu^+ cations bridging between two T2 clusters [81].

The diamond-type lattice is very common for framework structures formed from supertetrahedral clusters. With T2 clusters, amines or ammonium cations are usually big enough to fill the framework cavity. As a result, the interpenetration of two identical lattices does not usually occur. With larger clusters, charge-balancing organic amines are often not enough to fill the extra-framework space and the double-diamond type structure becomes more common.

In addition to the single-diamond type lattice, other types of framework structures are possible. One compound, Dabco-MnGS-SB1 with a formula of $\text{MnGe}_4\text{S}_{10}\cdot\text{C}_6\text{H}_{14}\text{N}_2\cdot 3\text{H}_2\text{O}$, has a framework structure in which T1 and T2 clusters alternate to form the zeolite ABW-type topology with a ring size of 12 tetrahedral atoms [82].

While the use of M^{2+} and M^+ cations have led to a number of open framework sulfides, they could have negative effects too. These low-charged metal sites could lower the thermal stability of the framework. The destabilizing effect of divalent cations (e.g. Co^{2+} , Mn^{2+}) in porous aluminophosphates is well known. However, unlike in phosphates, it is difficult to study the destabilizing effect of low-charged cations in open framework sulfides because the incorporation of low-charged cations in sulfides changes both chemical composition and framework type.

4.3 Sulfides with trivalent metal cations

In late 1990s, a new direction appeared when Parise, Yaghi and their coworkers reported several open framework indium sulfides [65,83]. The In-S composition is quite unique because no oxide open frameworks with similar compositions were known before. In fact, the In-O-In and Al-O-Al linkages are not expected to occur in

oxides with four-connected, three-dimensional structures. Fortunately, such a restriction does not apply to open framework sulfides.

An interesting structural feature in the In-S system is the occurrence of T3 clusters, $[\text{In}_{10}\text{S}_{18}]^{6-}$. A T3 cluster has both bi- and tri-coordinated sulfur sites. The lower charge of In^{3+} compared to Ge^{4+} and Sn^{4+} makes it possible to form tri-coordinated sulfur sites. Through the sharing of all corner sulfur atoms, open framework materials with several different framework topologies have been made. These include DMA-InS-SB1 (T3 double-diamond type) [83], ASU-31 (T3-decorated sodalite net), ASU-32 (T3-decorated CrB_4 type) [65], and ASU-34 (T3 single-diamond type) [84].

Very recently, Feng *et al.* synthesized a series of open framework materials based on T3 gallium sulfide clusters, $[\text{Ga}_{10}\text{S}_{18}]^{6-}$ [85]. Only the double-diamond type topology has been observed so far in the Ga-S system. In UCR-7GaS, T3 clusters are bridged by a sulfur atom (-S-) whereas in UCR-18GaS, one quarter of the inter-cluster linkage is through the trisulfide group (-S-S-S-).

So far, isolated T3 clusters, $[\text{In}_{10}\text{S}_{20}]^{10-}$ and $[\text{Ga}_{10}\text{S}_{20}]^{10-}$, have not been found yet even though isolated T2 clusters, $[\text{In}_4\text{S}_{10}]^{8-}$ and $[\text{Ga}_4\text{S}_{10}]^{8-}$, have been known for a while [86]. Regular supertetrahedral clusters larger than T3 have not been found in the binary In-S or Ga-S systems probably because tetrahedral sulfur atoms at the core of these clusters can not accommodate four trivalent metal cations because the positive charge surrounding the tetrahedral sulfur anion would be too high.

4.4 Sulfides with trivalent and mono- or divalent cations

To access clusters larger than T3, mono- or divalent cations need to be incorporated into the Ga-S or In-S compositions. Another motivation to incorporate mono- or divalent cations in the In-S or Ga-S synthesis conditions might be the desire to create new structures in which T3 clusters are joined together by mono- or divalent cations, in a manner similar to the assembly of $[\text{Ge}_4\text{S}_{10}]^{4-}$ clusters by mono- or divalent cations [73]. So far, mono- and divalent cations have only been observed to occur as part of a supertetrahedral cluster, not as linker units between clusters.

The first T4 cluster, $[\text{Cd}_4\text{In}_{16}\text{S}_{33}]^{10-}$, was synthesized by Yaghi, O'Keffee and coworkers in CdInS-44. In this compound, four Cd^{2+} cations are located around the core tetrahedral sulfur atom (Fig. 8). Because Cd^{2+} and In^{3+} are isoelectronic, it is difficult to distinguish Cd^{2+} and In^{3+} sites through the crystallographic refinement of X-ray diffraction data. Further evidences on the distribution of di- and trivalent cations in a T4 clusters came from UCR-1 and UCR-5 series of compounds that incorporate the first row transition metal cations such as Mn^{2+} , Fe^{2+} , Co^{2+} , and Zn^{2+} [87].

An exciting recent development is the synthesis of two superlattices (UCR-16 and UCR-17) consisting of T5 supertetrahedral clusters, $[\text{Cu}_5\text{In}_{30}\text{S}_{54}]^{13-}$ [67]. There are four tetrahedral core sulfur sites, each of which is surrounded by two In^{3+} and

two Cu^+ cations. One Cu^+ cation is located at the center of the T5 cluster and there is one Cu^+ cation on each face of the supertetrahedral cluster (Fig. 8).

Another interesting structural feature is the occurrence of hybrid superlattices. In UCR-19, T3 clusters $[\text{Ga}_{10}\text{S}_{18}]^{6-}$ and T4 clusters $[\text{Zn}_4\text{Ga}_{16}\text{S}_{33}]^{10-}$ alternate to form the double-diamond type superlattice [85]. In UCR-15, T3 clusters $[\text{Ga}_{10}\text{S}_{18}]^{6-}$ and pseudo-T5 clusters $[\text{In}_{34}\text{S}_{54}]^{6-}$ also alternate to form the double-diamond type superlattice [88]. The pseudo-T5 cluster is similar to the regular T5 cluster except that the core sulfur site is not occupied. The pseudo-T5 cluster has also been found with a different chemical composition in a layered superlattice with the framework composition of $[\text{Cd}_6\text{In}_{28}\text{S}_{54}]^{12-}$ [89].

4.5 Sulfides with tetravalent and trivalent cations

Open framework sulfides based on In-S and Ga-S compositions have open architectures and some have been shown to undergo ion exchange in solutions. However, to generate microporosity, it is necessary to remove a substantial amount of extra-framework species. Open framework sulfides such as indium or gallium sulfides generally do not have sufficient thermal stability to allow the removal of an adequate amount of extra-framework species to generate microporosity.

A general observation in zeolites is that the stability increases with the increasing $\text{Si}^{4+}/\text{Al}^{3+}$ ratio. It can be expected that the incorporation of tetravalent cations such as Ge^{4+} and Sn^{4+} into In-S or Ga-S compositions could lead to an increase in the thermal stability. Recently, Feng *et al.* reported a large family of chalcogenide zeolite analogs [46]. These materials were made by simultaneous triple substitutions of O^{2-} with S^{2-} or Se^{2-} , Si^{4+} with Ge^{4+} or Sn^{4+} , and Al^{3+} with Ga^{3+} or In^{3+} . All four possible $\text{M}^{4+}/\text{M}^{3+}$ combinations (Ga/Ge, Ga/Sn, In/Ge, and In/Sn) could be realized resulting in four zeolite-type topologies.

Based on the topological type, these materials are classified into four families denoted as UCR-20, UCR-21, UCR-22, and UCR-23. Each number refers to a series of materials with the same framework topology, but with different chemical compositions in either framework or extra-framework components. For example, UCR-20 can be made in all four $\text{M}^{4+}/\text{M}^{3+}$ combinations, giving rise to four sub-families denoted as UCR-20GaGeS, UCR-20GaSnS, UCR-20InGeS, and UCR-20InSnS. An individual compound is specified when both the framework composition and the type of extra-framework species are specified (e.g., UCR-20GaGeS-AEP, AEP = 1-(2-aminoethyl)piperazine).

The extra-large pore size and 3-rings are two interesting features. UCR-22 (Fig. 9) and UCR-23 have 24-ring and 16-ring windows whereas both UCR-20 (Fig. 9) and UCR-21 have 12-ring window. These inorganic frameworks are strictly 4-connected 3-dimensional networks commonly used for the systematic description of zeolite frameworks. Unlike known zeolite structure types, a key structural feature is the presence of the adamantane-cage shaped building unit, M_4S_{10} . The M_4S_{10} unit

consists of four 3-rings fused together. For materials reported here, the framework density defined as the number of T-atoms in 1000\AA^3 ranges from 4.4 to 6.5.

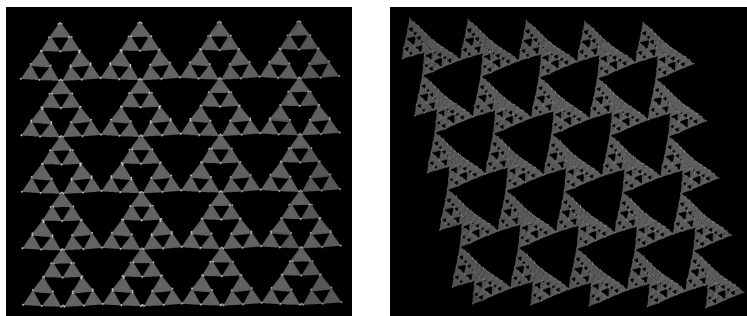


Figure 9. The three-dimensional framework of UCR-20 (left) and UCR-22 (right) families of sulfides.

Although these chalcogenides are strictly zeolite-type tetrahedral frameworks, it is possible to view them as decoration of even simpler tetrahedral frameworks. Here, each M_4S_{10} unit can be treated as a large artificial tetrahedral atom. With this description, UCR-20 has the decorated sodalite-type structure, in which a tetrahedral site in a regular sodalite net is replaced with a M_4S_{10} unit. UCR-21 has the decorated cubic ZnS type structure. UCR-23 has the decorated CrB_4 type network in which tetrahedral boron sites are replaced with M_4S_{10} units.

Upon exchange with Cs^+ ions, the percentage of C, H, and N in UCR-20GaGeS-TAEA was dramatically reduced. The exchanged sample remained highly crystalline as the original sample. The Cs^+ exchanged UCR-20GaGeS-TAEA displayed type I isotherm characteristic of a microporous solid. This sample has a high Langmuir surface area of $807\text{m}^2/\text{g}$ and a micropore volume of $0.23\text{cm}^3/\text{g}$ despite the presence of much heavier elements (Cs, Ga, Ge, and S) compared to aluminosilicate zeolites.

5 Microporous Metal-Organic Frameworks

Currently, the synthetic design of metal-organic frameworks (also known as coordination polymers) is a very active research area [90,91]. Many new microporous materials synthesized in the past several years belong to this family. Unlike zeolites that have an inorganic host framework, in metal-organic frameworks, the three-dimensional connectivity is established by linking metal cations or clusters with bidentate or multidentate organic ligands. The resulting frameworks are hybrid frameworks between inorganic and organic building units and should be

distinguished from microporous materials in which organic amines are encapsulated in the cavities of purely inorganic frameworks.

The development of metal-organic framework materials began in the early 1990s and was apparently an extension of the earlier work on three-dimensional cyanide frameworks [14,92,93]. In $K_2Zn_3[Fe(CN)_6]_2 \cdot xH_2O$ [94], octahedral Fe^{2+} and tetrahedral Zn^{2+} cations are joined together by linear CN^- groups to form a three-dimensional framework with cavities occupied by K^+ cations and water molecules. To generate large cavities, one method is to replace short CN^- ligands with large ligands such as nitriles [93], amines, and carboxylates [95]. A large variety of structural building units are possible with this approach. However, at the early stage of their development, metal-organic frameworks were plagued by problems such as lattice interpenetration and the low stability upon guest removal.

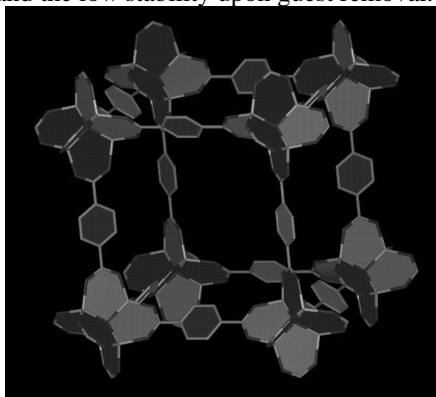


Figure 10. The framework of MOP-5, one of the first microporous metal-organic frameworks [98].

During the past several years, a substantial progress has occurred in the rational synthesis of these materials and a large number of metal-organic frameworks have been made that are capable of supporting microporosity as demonstrated by their gas sorption properties [96,97,98,99]. Such success was in part because of the use of rigid di- and tri-carboxylates and judicious selections of experimental conditions. It is worth noting that despite the wide selection of organic molecules that can serve as bridges between inorganic building units, new metal-organic frameworks are often made by changes in synthesis conditions such as pH, type of solvents, and temperature, instead of using new organic linker molecules. For example, $Zn(BDC)(DMF)(H_2O)$ (denoted as MOF-2, BDC = 1,4-benzenedicarboxylate, DMF = N, N'-dimethylformamide), $Zn_3(BDC)_3 \cdot 6CH_3OH$ (denoted as MOF-3), and $(Zn_4O)(BDC)_3(DMF)_8(C_6H_5Cl)$ (MOF-5) are all made from Zn^{2+} and BDC [100]. Their topological differences are caused by spacing-filling or structure-directing solvent molecules. These compounds clearly show the importance in controlling the synthesis conditions including the selection of solvent. This is somewhat similar to the synthesis in zeolites where the primary building units are the same (i.e., SiO_4 and

AlO₄ tetrahedra) in all structures and the difference in secondary building units and three-dimensional topologies is caused by extra-framework structure-directing agents.

Microporous metal-organic materials are complementary to oxide and chalcogenide based microporous materials such as zeolites. There are many fundamental differences between metal-organic materials and zeolites so that rather than competing with each other, they are expected to have different applications. For example, unlike zeolites and chalcogenides that usually have a negative framework, metal-organic frameworks (excluding cyanides) reported so far are usually positive or neutral. Therefore, while zeolites are cation exchangers, metal-organic frameworks can be anion exchangers.

For a given framework topology, the framework of a zeolite or a phosphate can often have a range of different charge density by varying the Si/Al ratio or doping Al³⁺ sites with divalent cations. The difference in the framework charge density in zeolites makes it possible to tune hydrophilicity or hydrophobicity of the framework. Metal-organic structures do not seem to have such flexibility in adjusting the framework charge density, however, the hydrophilicity or hydrophobicity in metal-organic frameworks is tunable by introducing different organic groups as shown in a series of compounds denoted as IRMOF-n [101].

Metal cations in metal-organic frameworks are usually transition metals, while in oxides and chalcogenides, main group elements dominate the framework cationic sites. Therefore, metal-organic frameworks can bind to guest molecules through coordinatively unsaturated transition metal sites [102,103]. Such interaction is not common with main group elements in zeolites or microporous phosphates, even though transition-metal doped zeolites or phosphates might contain active transition metal sites.

One potential with metal-organic frameworks is the possibility to form porous materials with pore size over 10Å by using large inorganic clusters or organic linkers. This potential is evidenced by the recent synthesis of a series of isorecticular MOFs denoted as IRMOF-n (n = 1 through 7, 8, 10, 12, 14, and 16) from different dicarboxylates [101]. These compounds have a calculated aperture size (also called free-diameter) from 3.8 to 19.1Å. IRMOFs also demonstrate the feasibility to have different organic groups in three-dimensional frameworks without a change in the framework topology.

The idea of using chiral structure-directing agents to direct the formation of chiral inorganic frameworks has been around for some time. However, few synthetic successes have been reported. Metal-organic frameworks provide a new opportunity in the design of chiral porous frameworks because chiral organic building units can be directly used for the construction of the framework. One recent example has shown this approach to be highly promising [104].

The recent synthetic success in producing microporous metal-organic frameworks has shifted some focus from the synthetic design to the potential

applications. One promising application of metal-organic frameworks is in the area of gas storage. Several metal-organic framework materials have been found to have a high capacity for methane storage [101,105,106]. For example, at 298K and 36atm, the quantity of methane adsorbed by IRMOF-6 is as high as 155cm^3 (STP)/ cm^3 , considerably higher than other crystalline porous materials such as zeolite 5A ($87\text{cm}^3/\text{cm}^3$). Such high adsorption capability is likely related to the more hydrophobic property of organic building units in these metal-organic frameworks, in addition to their high pore volumes and wide pore sizes.

In the following, we discuss in some more details metal-organic frameworks that either have a positive or neutral framework. Excluding cyanide frameworks, metal-organic frameworks with negative charges on the framework are far less common and remain to be explored in the future.

5.1 Cationic metal-organic frameworks

Cationic metal-organic frameworks were among the earliest to be studied. Some early examples of cationic metal-organic frameworks were formed between monovalent metal cations (Cu^+ or Ag^+) and neutral amines. Metal cations in these compounds can take different coordination geometry such as linear, trigonal or tetrahedral. Interestingly, ligands can also take different geometry. Examples of linear, trigonal, and tetrahedral ligands are 4,4'-bipyridine (4, 4'-bpy), 1,3,5-tricyanobenzene, and 4,4',4'',4'''-tetracyanotetraphenylmethane, respectively.

Examples of compounds with the cationic metal-organic frameworks include $\text{Ag}(4,4'\text{-bpy})\text{NO}_3$ [107] and $\text{Cu}(4,4'\text{-bpy})_2(\text{PF}_6)$ [108]. In $\text{Ag}(4,4'\text{-bpy})\text{NO}_3$, Ag^+ is coordinated to two 4,4'-bpy molecules in a nearly linear configuration and the three-dimensional framework is formed with the help of Ag-Ag (2.977\AA) interactions. In $\text{Cu}(4,4'\text{-bpy})_2(\text{PF}_6)$, Cu^+ ions have tetrahedral coordination and 4,4'-bpy behaves very much like linear CN- groups between two tetrahedral atoms. However, much larger void space forms as a result of longer length of 4,4'-bpy and such void space is reduced by the formation of four interpenetrating diamond-like frameworks in $\text{Cu}(4,4'\text{-bpy})_2(\text{PF}_6)$.

Some cationic frameworks have been found to display zeolitic properties such as ion exchange with anions in the solution. However, it has been difficult to remove extra-framework species to produce microporosity. Because of this limitation, there has been an increasing interest in using carboxylates as organic linkers. The current synthetic approach for the synthesis of carboxylate-based metal-organic frameworks usually gives rise to neutral frameworks discussed below.

5.2 Neutral metal-organic frameworks

In oxide and chalcogenide molecular sieves, a low framework charge generally means a high thermal stability. Therefore, neutral metal-organic frameworks should

provide the best opportunity for generating microporous metal-organic frameworks. In a metal-organic compound with a neutral framework, the host-guest interaction tends to be weaker than that in a solid with a charged framework. The weak host-guest interaction makes it possible to remove guest solvent molecules at relatively mild conditions. In addition, the neutral framework also tends to be more tolerant of the loss of neutral guest molecules.

Among the first metal-organic frameworks that showed zeolite-like microporosity through reversible gas sorption are MOF-2, $\text{Cu}_3(\text{BTC})_2(\text{H}_2\text{O})_x$ (denoted as HKUST-1 or Cu-BTC, BTC = 1,3,5-benzenetricarboxylate), and MOF-5 [97,98,109]. A key structural feature of Cu-BTC is the dimeric Cu-Cu (2.628Å) unit. A detailed investigation of sorption properties showed that Cu-BTC may be useable for separation of gas mixtures such as CO_2 -CO, CO_2 - CH_4 , and C_2H_4 - C_2H_6 mixtures [110].

The framework structure of MOF-5 is particularly simple with $(\text{Zn}_4\text{O})^{6+}$ clusters arranged at eight corners of a cube and linear BDC linkers located on edges of the cube (Fig. 10) [98]. The $(\text{Zn}_4\text{O})^{6+}$ cluster has a pseudo-octahedral connectivity because it connects to BDC through six edges of Zn_4 tetrahedra. Even more interesting is the fact that BDC molecules can be replaced by a series of different dicarboxylates without altering the framework topology [101]. This provides an elegant means of adjusting the pore size and framework functionality.

Neutral frameworks can also be prepared from neutral organic ligand. One such example is $[\text{CuSiF}_6(4,4'\text{-bpy})_2 \cdot 8\text{H}_2\text{O}]$ [106]. In this case, Cu^{2+} cations are linked into two-dimensional sheets by 4,4'-bpy ligands and these sheets are then linked into a three-dimensional framework by SiF_6^{2-} anions. This compound is microporous and has a high adsorption capacity for methane.

Metal-organic frameworks can also be created by a combined use of amines and carboxylates. For example, in $[\text{Zn}_4(\text{OH})_2(\text{fa})_3(4,4'\text{-bpy})_2]$ (fa = fumarate), dicarboxylate and diamine molecules work together to link $\text{Zn}_4(\text{OH})_2$ units into an interpenetrating three-dimensional framework [111]. Furthermore, carboxylate-substituted amines can simultaneously use COO- and N to bind to inorganic units to create an extended framework. One example is $\text{Cu}(\text{INA})_2 \cdot 2\text{H}_2\text{O}$ (INA = isonicotinate or pyridine-4-carboxylate) [112].

5.3 Metalloprophyrin-based metal-organic frameworks

A special class of ligands are porphyrins and metalloporphyrins. Metalloporphyrins can form either cationic or neutral frameworks depending on the nature of substituent groups. Two of the earliest examples are $\text{Cu}(\text{II})(\text{tpp})\text{Cu}(\text{I})\text{BF}_4(\text{solvent})$ and $\text{Cu}(\text{II})(\text{tcp})\text{Cu}(\text{I})\text{BF}_4 \cdot 17(\text{C}_6\text{H}_5\text{NO}_2)$ (tpp = 5,10,15,20-tetra(4-pyridyl)-21H,23H-porphine; tcp = 5,10,15,20-tetrakis(4-cyanophenyl)-21H,23H-porphine) [113]. In both cases, the framework is constructed from equal numbers of tetrahedral (Cu)

and square planar (Cu-tpp or Cu-tcp) centers. Neither of these two compounds is stable upon solvent removal.

A stable metalloporphyrin-based metal-organic framework was recently demonstrated by Suslick *et. al.* [114]. PIZA-1 with a formula of $[\text{Co(III)T}(\text{p-CO}_2\text{)PPCo(II)}_{1.5}(\text{C}_5\text{H}_5\text{N})_3(\text{H}_2\text{O})\cdot\text{C}_5\text{H}_5\text{N}]$ is formed from carboxylate-substituted tetraphenylporphyrins with cobalt ions. Because of the presence of carboxylate groups, the framework of PIZA-1 is neutral. It is apparent that the ability of transition metals (Cu and Co) to exist in different oxidation states helps the formation of these metalloporphyrin-based metal-organic frameworks.

No mixed valency occurs in SMTP-1 [115], a family of layered structures with a general formula of $[\text{M}(\text{tpp})_6]\cdot\text{G}$ ($\text{M} = \text{Co}^{2+}$, $\text{G} = 12\text{CH}_3\text{COOH}\cdot 12\text{H}_2\text{O}$; $\text{M} = \text{Mn}^{2+}$, $\text{G} = 60\text{H}_2\text{O}$; or $\text{M} = \text{Mn}^{2+}$, $\text{G} = 12\text{C}_2\text{H}_5\text{OH}\cdot 24\text{H}_2\text{O}$). SMTP-1 differs from the above metalloporphyrin-based structures. The metal cation in the center of the porphyrin ring is also coordinated to pyridyl groups of other tpp complexes, allowing the creation of an extended layer structure without the use of separate metal cations for crosslinking tpp complexes.

5.4 Metal-organic frameworks from oxide clusters

In metal-organic frameworks, the inorganic unit is often a single transition metal cation (sometimes with some coordinating solvent molecules attached). The diversity of metal-organic frameworks can be greatly increased if inorganic clusters are used as structural building units. The simplest situation is dinuclear units such as Ag_2 in $\text{Ag}(4,4'\text{-bpy})\text{NO}_3$ and Cu_2 in Cu-BTC [97,107]. The Zn_2 (2.940Å) unit is found in MOF-2. Clusters containing three or four metal cations are also known. For example, a chiral metal-organic framework called D-POST-1 contains the Zn_3O unit in which the oxygen atom is located at the center of the Zn_3 triangle [104]. Similarly, the Zn_4O unit containing tetrahedrally coordinated oxygen anions was recently found in MOF-5 and IRMOF series of compounds. Much larger units (e.g., Zn_8SiO_4) have also been reported [116,117,118]. In many cases, these inorganic clusters do not occur in the starting materials and they are formed *in situ* during the synthesis of metal-organic frameworks.

5.5 Metal-organic frameworks from chalcogenide clusters

As shown above, the use of organic multidentate ligands to organize inorganic species is an effective method to prepare porous solids with tunable pore sizes. However, inorganic building units are generally limited to individual metal ions (e.g., Zn^{2+}) or their oxide clusters (e.g., Zn_4O^{6+}). To expand applications of porous materials beyond traditional areas such as adsorption and catalysis, metal-organic frameworks based on semiconducting chalcogenide nanoclusters are highly desirable. Recently, Feng *et. al* reported the organization of the cubic $[\text{Cd}_8(\text{SPh})_{12}]^{4+}$

clusters by in-situ generated tetradentate dye molecules [119]. The structure consists of three-dimensional inorganic-organic open framework with large uni-dimensional channels. The combination of dye molecules and the inorganic cluster unit in the same material creates a synergistic effect that greatly enhances the emission of the inorganic cluster at 580nm. Such an emission can be excited by an unusually broad spectral range down to the UV, which is believed to result from the absorption of dye molecules and the subsequent energy transfer.

6 Extra-large Pore Crystalline Molecular Sieves

Thus far, an extra-large pore material is conveniently understood as those having a ring size of over 12 tetrahedral atoms [120]. In zeolites, the maximum pore size of a 12-ring pore is about 8Å. The recent progress in metal-organic frameworks has made it possible to obtain porous materials with pore size larger than 8Å by using larger organic linkers rather than by forming pores with more than 12 metal cations.

Among silicates, the extra-large pore has only been found in two high silica zeolites and one beryllosilicate. The first extra-large pore zeolite (UTD-1) was reported in 1996 (Fig. 11) [121,122]. UTD-1 (DON) was synthesized using bis(pentamethylcyclopentadienyl) cobalticinium cations and has a ring size of 14 tetrahedral atoms. It has a one-dimensional channel system with the approximate free diameter of 7.5 x 10Å for the 14-ring pore. Another extra-large pore zeolite (CIT-5) was reported in 1997 [123,124]. Like UTD-1, CIT-5 (CFI) also has a ring size of 14 tetrahedral atoms with a one-dimensional channel system. The effective pore size (6.4Å measured using the Horvath-Kawazoe method) of CIT-5 is similar to that of one-dimensional 12-ring channel in SSZ-24 (AFI) [125]. Very recently, a hydrated potassium beryllosilicate called OSB-1 (OSO) was found to have an extra-large pore size of 14 tetrahedral atoms [30].

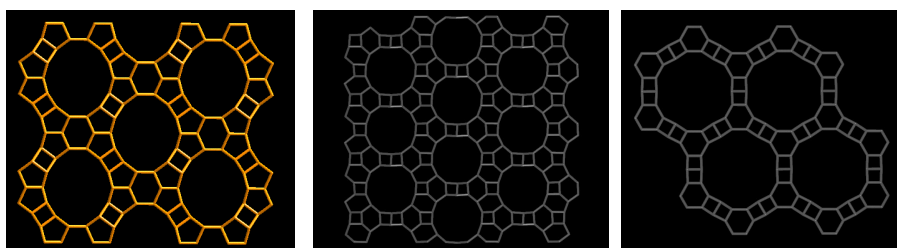


Figure 11. (left) The three-dimensional framework of UTD-1 (DON) elliptical 14-ring windows; Reprinted with permission from <http://www.iza-structures.org/> and reference [30]. (middle) the three-dimensional framework of AlPO₄-8 (AET) showing 14-ring windows (right) the three-dimensional framework of VPI-5 (VFI) 18-ring windows.

Most extra-large pore materials such as cacoxenite, VPI-5, cloverite, and JDF-20 are found in phosphates [15,126,127,128]. While the ring size of only 14 tetrahedral atoms is known in silicates, extra-large pore phosphates come with various ring sizes including 14, 16, 18, 20, and 24. Structures of these phosphates sometimes deviate from those of typical zeolites in several aspects including framework interruptions by terminal OH, F, or H₂O groups and non-tetrahedral coordination. These deviations tend to lower the thermal stability of extra-large pore phosphates. On the other hand, it is often because of these deviations that extra-large pores are formed.

The first synthetic extra-large pore phosphate is VPI-5 with one-dimensional channel defined by 18 oxygen atoms (Fig. 11) [15]. Unlike most aluminophosphate molecular sieves, VPI-5 is a hydrated aluminophosphate and does not contain any organic structure-directing agent. Under suitable heating conditions, VPI-5 can be recrystallized into another extra-large pore phosphate called AlPO₄-8 (AET) with a 14-ring pore size (Fig. 11) [129].

Among the most recent development in the area of microporous phosphates is the synthesis of two extra-large pore nickel phosphates denoted as VSB-1 and VSB-5 [130,131]. Similar to VPI-5, Both VSB-1 and VSB-5 are hydrates and organic amines used in the syntheses were not occluded into the final structures. VSB-1 and VSB-5 have one-dimensional 24-ring channels and both of them have good thermal stability. The nitrogen adsorption shows the type I isotherms typical of a microporous material.

The synthesis of VPI-5, VSB-1, and VSB-5 demonstrates that neither large nor small organic structure-directing agents are essential for the preparation of extra-large pore sizes. The formation of different pore sizes likely depends on types of small structural units that eventually come together to create the framework and the pore. The structural and synthetic factors that affect the formation of these small structural units may have a substantial effect on the creation of extra-large pore materials.

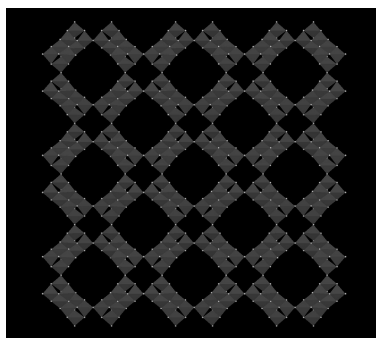


Figure 12. The three-dimensional framework of UCR-23 family of sulfides showing 16-ring channels.

One strategy for the preparation of the extra-large pore size is to generate a large number of small rings, particularly 3-rings. Because the average ring size in a three-dimensional four-connected net is approximately 6, the presence of small rings will be accompanied by large or extra-large rings so that the average ring size will be about 6 [132]. This strategy can be illustrated with the recent discovery of a large family of extra-large pore sulfides.

Because of the large T-S distances and small T-S-T angles, 3-rings often occur in open framework metal sulfides. Correspondingly, large pore and extra-large pore sizes are typically structural features in sulfides. For example, UCR-20, UCR-21, and UCR-22, and UCR-23 consist of adamantane-shaped clusters (T_4S_{10}) with 3-rings. While both UCR-20 and UCR-21 are large-pore sulfides, UCR-23 has three-dimensional intersecting 16-, 12-, and 12-ring channels (Fig. 12) and UCR-22 consists of interpenetrating three-dimensional framework with 24-ring window size.

Other strategies for increasing the pore size include the use of large structural building units such as clusters and the use of long linker molecules between two structural building units. For example, the use of chalcogenide supertetrahedral clusters as large artificial tetrahedral atoms has resulted in a number of three-dimensional frameworks with extra-large pore sizes. Equally successful is the use of dicarboxylates as molecular linkers to join together metal cations or their clusters to generate a series of metal-organic frameworks with pore sizes $> 10\text{\AA}$. By using different supertetrahedral clusters and carboxylates, the pore size of the resulting open framework materials can be tuned.

7 Acknowledgement

We thank Dr. Qisheng Huo for critical evaluation of this manuscript and Nanfeng Zheng for assistance with figures.

References

1. Rouquerol J., Avnir D., Fairbridge C. W., Everett D. H., Haynes J. H., Pernicone N., Ramsay J. D. F., Sing K. S. W. and Unger, K. K. Recommendations for the characterization of porous solids, *Pure Appl. Chem.* **66** (1994) pp. 1739-58.
2. McCusker L. B., Liebau F. and Engelhardt G., Nomenclature of structural and compositional characteristics of ordered microporous and mesoporous materials with inorganic hosts (IUPAC recommendations 2001), *Pure Applied Chem.* **73** (2001) pp. 381-394.
3. Barton T. J., Bull L. M., Klemperer W. G., Loy D. A. McEnaney B., Misono M., Monson P. A., Pez G., Scherer B., Vartuli J. C. and Yaghi O. M., Tailored Porous Materials, *Chem. Mater.* **11** (1999) pp. 2633-2656.
4. Weitkamp J., Zeolites and catalysis, *Solid State Ionics* 131 (2000) pp. 175-188.

-
5. Smith J. V., Definition of a Zeolite, *Zeolites* **4** (1984) pp. 309-310.
 6. Foley, H. C., Carbogenic molecular sieves: synthesis, properties and applications, *Micro. Mater.* **4** (1995) 407-433.
 7. Barrer R. M., Synthesis of a zeolitic mineral with chabazitelike sorptive properties, *J. Chem. Soc.* (1948) pp. 127-132.
 8. Milton R. M., Molecular sieve science and technology. A historical perspective, *ACS Symposium Series* (1989), **398** (Zeolite Synth.), pp. 1-10.
 9. Argauer R. J. and Landolt G. R. Crystalline Zeolite ZSM-5 and Method of Preparing the Same, US Patent 3,702,886, 1972.
 10. Flanigen E. M., Bennett J. M., Grose R. W., Cohen J. P., Patton R. L., Kirchner R. M. and Smith, J. V. Silicalite, a new hydrophobic crystalline silica molecular sieve, *Nature* **271** (1978) pp. 512-516.
 11. Wilson S. T., Lok B. M., Messina C. A., Cannan T. R. and Flanigen E. M., Aluminophosphate Molecular Sieves: A New Class of Microporous Crystalline Inorganic Solids, *J. Am. Chem. Soc.* **104** (1982) pp. 1146-1147.
 12. Wilson S. T., Lok B. M., Messina C. A., Cannan T. R. and Flanigen, E. M., Aluminophosphate molecular sieves: a new class of microporous crystalline inorganic solids, *ACS Symposium Series* (1983), **218** (Intrazeolite Chem.), pp. 79-106.
 13. Cheetham A. K., Ferey G. and Loiseau T., Open-Framework Inorganic Materials, *Angew. Chem. Int. Ed.* **38** (1999) pp. 3268-3292.
 14. Bowes C. L. and Ozin G. A., Self-Assembling Frameworks: Beyond Microporous Oxides, *Adv. Mater.* **6** (1996) pp. 13-28.
 15. Davis M. E., Saldarriaga C., Montes C., Garces J. and Crwoder C., A molecular sieve with eighteen-membered rings, *Nature* **331** (1988) pp. 698-699.
 16. Davis M. E. Ordered porous materials for emerging applications, *Nature* **147** (2002) pp. 813-821.
 17. Evans O. R., Lin W., Crystal Engineering of NLO Materials Based on Metal-Organic Coordination Networks, *Acc. Chem. Res.* **35** (2002) pp. 511-522.
 18. Davis M. E. and Lobo R. F., Zeolite and Molecular Sieve Synthesis, *Chem. Mater.* **4** (1992) pp. 756-768.
 19. Davis M. E., New Vistas in Zeolite and Molecular Sieve Catalysis, *Acc. Chem. Res.* **26** (1993) pp. 111-115.
 20. Breck D. W., *Zeolite Molecular Sieves*, Wiley, New York, 1974.
 21. Barrer R. M., *Zeolites and Clay Minerals as Sorbents and Molecular Sieves*, Academic Press, 1978.
 22. Dyer A., *An Introduction to Zeolite Molecular Sieves*, John Wley & Sons, 1988.
 23. van Bekkum H., Flanigen E. M. and Jansen J. C., *Studies in Surface Science and Catalysis*, Vol. **58** (*Introduction to Zeolite Science and Practice*) Elsevier, New York, 1991.

-
24. Jansen J. C., Stocker M., Karge H. G. and Weitkamp, *Studies in Surface Science and Catalysis*, Vol. **85** (*Advanced Zeolite Science and Applications*), Elsevier, 1994.
 25. Atwood J. L., Davies J. E. D., MacNicol D. D. and Vogtle F., *Comprehensive Supramolecular Chemistry*, Vol. **7** (*Solid-State Supramolecular Chemistry: Two- and Three-Dimensional Inorganic Networks*, eds. Altermann G. and Bein T.), Elsevier, 1996.
 26. Fricke R., Kosslick H., Lischke G. and Richter M., Incorporation of Gallium into Zeolites: Syntheses, Properties and Catalytic Application. *Chem. Rev.* **100** (2000) pp. 2303-2405.
 27. Saxton R. J., Crystalline microporous titanium silicates, *Topics in Catalysis* **9** (1999) pp. 43-57.
 28. Rocha J. and Anderson M. W. Microporous Titanosilicates and other Novel Mixed Octahedral-Tetrahedral Framework Oxides, *Eur. J. Inorg. Chem.* (2000) pp. 801-818.
 29. Loewenstein W., The distribution of aluminum in the tetrahedra of silicates and aluminates, *Am. Mineralogist* **39**, (1954), pp. 92-96.
 30. Baerlocher Ch., Meier W. M., Olson D. H. *Atlas of Zeolite Framework Types*, 2001, Elsevier.
 31. Smith J. V., Topochemistry of zeolites and related materials. 1. Topology and geometry, *Chem. Rev.* **88** (1988), pp. 149-82.
 32. Gier T. E., Bu X., Feng P. and Stucky G. D., Synthesis and organization of zeolite-like materials with three-dimensional helical pores, *Nature* **395** (1998), pp. 154-157.
 33. Zones S. I., Davis M. E., Zeolite materials: Recent discoveries and future prospects. *Curr. Opin. Solid State Mater. Sci.* **1** (1996) pp. 107-117.
 34. Kessler H., Patarin J., Schott-Daric C., in The opportunities of the fluoride route in the synthesis of microporous materials, *Studies in Surface Science and Catalysis* (1994), **85**(*Advanced Zeolite Science and Applications*), pp. 75-113.
 35. Kuperman A., Nadimi S., Oliver S., Ozin G. A., Garces J. M., Olken M. M., Non-aqueous synthesis of giant crystals of zeolites and molecular sieves, *Nature* **365** (1993) pp. 239-242.
 36. Cambor M. A., Villaescusa L. A., Diaz-Cabanas M. J., Synthesis of all-silica and high-silica molecular sieves on fluoride media, *Topics in Catalysis* **9** (1999) pp. 59-76.
 37. Cambor M. A., Corma A., Lightfoot P., Villaescusa L. A., Wright P. A., Synthesis and structure of ITQ-3, the first pure silica polymorph with a two-dimensional system of straight eight-ring channels, *Angew. Chem. Int. Ed.* **36** (1997) pp. 2659-2661.

-
38. Barrett A., Cambor M. A., Corma A., Jones H. and Villaescusa, Structure of ITQ-4, a New Pure Silica Polymorph Containing Large Pores and a Large Void Volume, *Chem. Mater.* **9** (1997) pp. 1713-1715.
 39. Villaescusa L., Barrett P. and Cambor M. A., ITQ-7: A new Pure Silica Polymorph with a Three-Dimensional System of Large Pore Channels, *Angew. Chem. Int. Ed.* **38** (1999) pp. 1997-2000.
 40. Corma A., Diaz-Cabanas M. J., Martinez-Triguero J., Rey F. and Rius J., A large-cavity zeolite with wide pore windows and potential as an oil refining catalyst, *Nature* **418** (2002) pp. 514-517.
 41. Blasco T., Corma A., Diaz-Cabanas M. J., Rey F., Vidal-Moya J. A. and Zicovich-Wilson C. M., Preferential Location of Ge in the Double Four-Membered Ring Units of ITQ-7 Zeolite, *J. Phys. Chem. B* **106** (2002) pp. 2634-2642.
 42. Corma A., Navarro M. T., Rey F. and Valencia S., Synthesis of pure polymorph C of Beta Zeolite in a fluoride-free system, *Chem. Commun.* (2001) pp. 1486-1487.
 43. Bu X., Feng P. and Stucky G. D. Novel Germanate Zeolite Structures with 3-Rings. *J. Am. Chem. Soc.* **120** (1998) pp. 11204-11205.
 44. O'Keeffe M., Yaghi O. M., Germanate zeolites: contrasting the behavior of germanate and silicate structures built from cubic T8O20 units (T = Ge or Si). *Chem. Eur. J.* **5** (1999) pp. 2796-2801.
 45. Martin J. D. and Greenwood K. B., Halozeotypes: A New Generation of Zeolite-Type Materials, *Angew. Chem.* **36** (1997) pp. 2072-2075.
 46. Zheng N., Bu X., Wang B., Feng P., Microporous and Photoluminescent Chalcogenide Zeolite Analogs, *Science* **298** (2002) pp. 2366-2369.
 47. Breck D. W., Eversole W. G., Milton R. M., New synthetic crystalline zeolites, *J. Am. Chem. Soc.* **78** (1956) pp. 2338-9.
 48. Effenberger H., Giester G., Krause W. and Bernhardt H.-J. Tschortnerite, a copper-bearing zeolite from the Bellberg volcano, Eifel, Germany, *Am. Mineralogist* **83** (1998) pp. 607-617.
 49. Bu X., Feng P., Stucky G. D. Large-cage zeolite structures with multidimensional 12-ring channels, *Science* **278** (1997) pp. 2080-2085.
 50. Feng P., Bu X. and Stucky G. D. Hydrothermal syntheses and structural characterization of zeolite analog compounds based on cobalt phosphate, *Nature* **388** (1997) pp. 735-741.
 51. Bennett J. M., Cohen J. P., Flanigen E. M., Pluth J. J., Smith J. V., Crystal structure of tetrapropylammonium hydroxide-aluminum phosphate Number 5, *ACS Symposium Series* **218** (1983) (*Intrazeolite Chem.*), pp. 109-118.
 52. Lok B. M., Messina C. A., Patton R. L., Gajek R. T., Cannan T. R. and Flanigen E. M., Silicoaluminophosphate Molecular Sieves: Another New Class

-
- of Microporous Crystalline Inorganic Solids, *J. Am. Chem. Soc.* **106** (1984) pp. 6092-6093.
53. Wilson S. T. and Flanigen E. M., Synthesis and Characterization of Metal Aluminophosphate Molecular Sieves, in *Zeolite Synthesis, ACS Symposium Series* **398** (1989), pp. 329-345, Eds. Occelli M. L. and Robson H. E., American Chemical Society, Washington DC.
 54. Chen J., Jones R., Natarajan S., Hursthouse M. B. and Thomas J. M., A Novel Open-Framework Cobalt Phosphate Containing a tetrahedral Coordinated Cobalt(II) Center: $\text{CoPO}_4 \cdot 0.5\text{C}_2\text{H}_{10}\text{N}_2$, *Angew. Chem. Int. Ed. Engl.* **33** (1994) pp. 639-640.
 55. Xiao F., Qiu S., Pang W., Xu R. New Development in Microporous Materials, *Adv. Mater.* **11** (1999) 1091-1099.
 56. Bibby D. M. and Dale M. P., Synthesis of silica-sodalite from nonaqueous systems, *Nature* **317** (1985) pp. 157-8.
 57. Soghomonian V., Chen Q., Haushalter R. C., Zubieta J. and O'Connor C. J., An Inorganic Double Helix: Hydrothermal Synthesis, Structure, and Magnetism of Chiral $[(\text{CH}_3)_2\text{NH}_2]\text{K}_4[\text{V}_{10}\text{O}_{10}(\text{H}_2\text{O})_2(\text{OH})_4(\text{PO}_4)_7] \cdot 4\text{H}_2\text{O}$, *Science* **259** (1993) pp. 1596-1599.
 58. Chippindale A. M., Walton, R. I. Synthesis and characterization of the first three-dimensional framework cobalt-gallium phosphate $[\text{C}_5\text{H}_5\text{NH}]^+[\text{CoGa}_2\text{P}_3\text{O}_{12}]^-$, *J. Chem. Soc., Chem. Commun.* (1994) pp. 2453-2454.
 59. Cowley A. R., Chippindale A. M., Synthesis and characterization of $[\text{C}_4\text{NH}_{10}]^+[\text{CoGaP}_2\text{O}_8]^-$, a CoGaPO analog of the zeolite gismondine, *Chem. Commu.* (1996) pp. 673-674.
 60. Chippindale A. M., Cowley A. R., CoGaPO-5: Synthesis and crystal structure of $(\text{C}_6\text{N}_2\text{H}_{14})_2[\text{Co}_4\text{Ga}_5\text{P}_9\text{O}_{36}]$, a microporous cobalt-gallium phosphate with a novel framework topology, *Zeolites* **18** (1997) pp. 176-181.
 61. Bedard R. L., Wilson S. T., Vail L. D., Bennett J. M. and Flanigen, E. M. The next generation: synthesis, characterization, and structure of metal sulfide-based microporous solids in *Zeolites: Facts, Figures, Future. Proceedings of the 8th International Zeolite Conference*, (1989) pp. 375-387. eds. Jacobs P. A. and van Santen, R. A. Elsevier, Amsterdam.
 62. Feng P., Zhang T., Bu X., Arsenate Zeolite Analogues with 11 Topological Types, *J. Am. Chem. Soc.* **123** (2001) pp. 8608-8609.
 63. Bu X., Feng P., Gier T. E., Zhao D. and Stucky G. D., Hydrothermal Synthesis and Structural Characterization of Zeolite-like Structures Based on Gallium and Aluminum Germanates, *J. Am. Chem. Soc.* **120** (1998) pp. 13389-13397.
 64. Li H. and Yaghi O. M., Transformation of Germanium Dioxide to Microporous Germanate 4-Connected Nets, *J. Am. Chem. Soc.* **120** (1998) pp. 10569-10570.

-
65. Li H., Laine A., O'Keeffe M., Yaghi O. M., Supertetrahedral Sulfide Crystals with Giant Cavities and Channels, *Science* **283** (1999) pp. 1145-1147.
66. Cahill C. L., Parise J. B., On the formation of framework indium sulfides, *J. Chem. Soc. Dalton Trans.* (2000) pp. 1475-1482.
67. Bu X., Zheng N., Li Y., Feng P., Pushing Up the Size Limit of Chalcogenide Supertetrahedral Clusters: Two- and Three-Dimensional Photoluminescent Open Frameworks from $(\text{Cu}_5\text{In}_{30}\text{S}_{54})^{13-}$ Clusters, *J. Am. Chem. Soc.* **124** (2002) pp. 12646-12647.
68. Dance I. G., Choy A., Scudder M. L., Syntheses, Properties, and Molecular and Crystal Structures of $(\text{Me}_4\text{N})_4[\text{E}_4\text{M}_{10}(\text{SPh})_{16}]$ (E = S, Se; M = Zn, Cd): Molecular Supertetrahedral Fragments of the Cubic Metal Chalcogenide Lattice, *J. Am. Chem. Soc.* **106** (1984) pp. 6285-6295.
69. Dance I. And Fisher K., Metal Chalcogenide Cluster Chemistry, in *Prog. Inorg. Chem.* (1994) pp. 637-803, Ed. Karlin K. D., John Wiley & Sons, Inc.
70. Conradson T., Dadachov M. S. and Zou X. D., "Synthesis and structure of $(\text{Me}_3\text{N})_6[\text{Ge}_{32}\text{O}_{64}] \cdot (\text{H}_2\text{O})_{4.5}$, a thermally stable novel zeolite with 3D interconnected 12-ring channels, *Micro. Meso. Mater.* **41** (2000) pp. 183-191.
71. Krebs B., Thio- and Seleno-Compounds of Main Group Elements- Novel Inorganic Oligomers and Polymers, *Angew. Chem. Int. Ed. Engl.* **22** (1983) pp. 113-134.
72. Pivan J. Y., Achak O. A., Louer M. and Louer D., The Novel Thiogermanate $[(\text{CH}_3)_4\text{N}]_4\text{Ge}_4\text{S}_{10}$ with a High Cubic Cell Volume. Ab Initio Structure Determination from Conventional X-ray Powder Diffraction, *Chem. Mater.* **6** (1994) pp. 827-830.
73. Yaghi O. M., Sun Z., Richardson D. A. and Loy T. L. Directed Transformation of Molecules to Solids: Synthesis of a Microporous Sulfide from Molecular Germanium Sulfide Cages, *J. Am. Chem. Soc.* **116** (1994) pp. 807-808.
74. Nellis D. M., Ko Y., Tan K., Koch S. and Parise J. B., A One-dimensional Germanium Sulfide Polymer Akin to the Ionosilicates: Synthesis and Structural Characterization of DPA-GS-8, $\text{Ge}_4\text{S}_9(\text{C}_3\text{H}_7)_2\text{NH}_2(\text{C}_3\text{H}_7)\text{NH}_2(\text{C}_2\text{H}_5)$, *J. Chem. Soc., Chem. Commun.* (1995) pp. 541-542.
75. MacLachlan M. J., Petrov S., Bedard R. L., Manners I. And Ozin G. A., Synthesis and Crystal Structure of δ -GeS₂, the First Germanium Sulfide with an Expanded Framework Structure, *Angew. Chem. Int. Ed.* **37** (1998) pp. 2076-2079.
76. Jiang T. and Ozin G. O., New directions in tin sulfide chemistry, *J. Mater. Chem.* **8** (1998) pp. 1099-1108.
77. Parise J. B. and Ko Y., Material Consisting of two Interwoven 4-Connected Networks: Hydrothermal Synthesis and Structure of $[\text{Sn}_5\text{S}_9\text{O}_2][\text{NH}(\text{CH}_3)_3]_2$, *Chem. Mater.* **6** (1994) pp. 718-720.

78. Schiwy W., Krebs B. $\text{Sn}_{10}\text{O}_4\text{S}_{20}^{8-}$: A New Type of Polyanion, *Angew. Chem. Int. Ed.* **14** (1975) p. 436.
79. Achak O., Pivan J. Y., Maunaye M., Louer M. and Louer D. The *ab initio* structure determination of $[(\text{CH}_3)_4\text{N}]_2\text{Ge}_4\text{MnS}_{10}$ from X-ray powder diffraction data, *J. Alloys Compounds* **219** (1995) pp. 111-115.
80. Achak, O., Pivan J. Y., Maunaye M., Louer M., Louer D., Structure Refinement by the Rietveld Methods of the Thiogermanates $[(\text{CH}_3)_4\text{N}]_2\text{MGe}_4\text{S}_{10}$ (M=Fe, Cd), *J. Solid State Chem.* **121** (1996) pp. 473-478.
81. Tan K., Darovsky A. and Parise J. B., Synthesis of a Novel Open-Framework Sulfide, $\text{CuGe}_2\text{S}_5 \cdot (\text{C}_2\text{H}_5)_4\text{N}$, and Its Structure Solution Using Synchrotron Imaging Plate Data, *J. Am. Chem. Soc.* **117** (1995) pp. 7039-7040.
82. Cahill C. L. and Parise J. B. Synthesis and Structure of $\text{MnGe}_4\text{S}_{10} \cdot (\text{C}_6\text{H}_{14}\text{N}_2) \cdot 3\text{H}_2\text{O}$: A Novel Sulfide Framework Analogous to Zeolite Li-A(BW), *Chem. Mater.* **9** (1997) pp. 807-811.
83. Cahill C. L., Ko Y. and Parise J. B., A Novel 3-Dimensional Open Framework Sulfide Based upon the $[\text{In}_{10}\text{S}_{20}]^{10-}$ Supertetrahedron: DMA-InS-SB1, *Chem. Mater.* **10** (1998) pp. 19-21.
84. Li H., Eddaoudi M., Laine A., O'Keeffe M. and Yaghi O. M., Noninterpenetrating Indium Sulfide Supertetrahedral Cristobalite Framework, *J. Am. Chem. Soc.* **121** (1999) pp. 6096-6097.
85. Zheng N., Bu X., Feng P., Nonaqueous Synthesis and Selective Crystallization of Gallium Sulfide Clusters into Three-Dimensional Photoluminescent Superlattices, *J. Am. Chem. Soc.* **125** (2003) pp. xxxx-xxxx.
86. Krebs B., Voelker D., Stiller K., Novel Adamantane-like Thio- and Selenoanions from Aqueous Solution: $\text{Ga}_4\text{S}_{10}^{8-}$, $\text{In}_4\text{S}_{10}^{8-}$, $\text{In}_4\text{Se}_{10}^{8-}$, *Inorg. Chim. Acta* **65** (1982) pp. L101-L102.
87. Wang C., Li Y., Bu X., Zheng N., Zivkovic O., Yang C., Feng P. Three-Dimensional Superlattices Built from $(\text{M}_4\text{In}_{16}\text{S}_{33})^{10-}$ (M = Mn, Co, Zn, Cd) Supertetrahedral Clusters, *J. Am. Chem. Soc.* **123** (2002) pp. 11506-11507.
88. Wang C., Bu X., Zheng N., Feng P., Nanocluster with One Missing Core Atom: A Three-Dimensional Hybrid Superlattice Built from Dual-Sized Supertetrahedral Clusters, *J. Am. Chem. Soc.* **124** (2002) pp. 10268-10269.
89. Su W., Huang X., Li J. and Fu H., Crystal of Semiconducting Quantum Dots Built on Covalently Bonded T5 $[\text{In}_{28}\text{Cd}_6\text{S}_{54}]^{-12}$: The Largest Supertetrahedral Clusters in Solid State, *J. Am. Chem. Soc.* **124** (2002) pp. 12944-12945.
90. Ferey, G., Microporous Solids: From Organically Templated Inorganic Skeletons to Hybrid Frameworks...Ecumenism in Chemistry, *Chem. Mater.* **13** (2001) pp. 3084-3098.
91. Batten S. R., Coordination polymers, *Cur. Opin. Solid State Mater. Sci.* **5** (2001) pp. 107-114.

-
92. Hoskins B. F. and Robson R., Design and Construction of a New Class of Scaffolding-like Materials Comprising Infinite Polymeric Frameworks of 3D-Linked Molecular Rods. A Reappraisal of the $\text{Zn}(\text{CN})_2$ and $\text{Cd}(\text{CN})_2$ structures and the Synthesis and Structures of the Diamond-Related Frameworks $[\text{N}(\text{CH}_3)_4][\text{Cu}^{\text{I}}\text{Zn}^{\text{II}}(\text{CN})_4]$ and $\text{Cu}^{\text{I}}[4,4',4'',4''']$ -tetracyanotetraphenylmethane] $\text{BF}_4 \cdot x\text{C}_6\text{H}_5\text{NO}_2$, *J. Am. Chem. Soc.* **112** (1990) pp. 1546-1554.
93. Gardner G. B., Venkataraman D., Moore J. S., Lee S., Spontaneous assembly of a hinged coordination network, *Nature* **374** (1995) pp. 792-795.
94. Gravereau P. P. and Hardy E. G. A., Les Hexacyanoferrates Zeolithiques: Structure Cristalline de $\text{K}_2\text{Zn}_3[\text{Fe}(\text{CN})_6]_2 \cdot x\text{H}_2\text{O}$, *Acta Cryst.* **B35** (1979) pp. 2843-2848.
95. Yaghi O. M. Li G. and Li H., Selective binding and removal of guests in a microporous metal-organic framework, *Nature* **378** (1995) pp. 703-706.
96. Li H., Eddaoudi M., Groy T. L. and Yaghi O. M., Establishing Microporosity in Open Metal-Organic Frameworks: Gas Sorption Isotherm for $\text{Zn}(\text{BDC})$ (BDC = 1,4-Benzenedicarboxylate), *J. Am. Chem. Soc.* **120** (1998) pp. 8571-8572.
97. Chui, S. S. -Y, Lo S. M. -F, Charmant J. P. H., Orpen A. G. and Williams I. D. A Chemically Functionalizable Nanoporous Material $[\text{Cu}_3(\text{TMA})_2(\text{H}_2\text{O})_3]_n$, *Science* **283** (1999) pp. 1148-1150.
98. Li H., Eddaoudi M., O'Keeffe M., Yaghi O. M., Design and synthesis of an exceptionally stable and highly porous metal-organic framework, *Nature* **402** (1999) pp. 276-279.
99. Chen B., Eddaoudi M., Hyde S. T., O'Keeffe M. and Yaghi O. M., Interwoven Metal-Organic Framework on a Periodic Minimal Surface with Extra-Large Pores, *Science* **291** (2001) pp. 1021-1023.
100. Eddaoudi M., Li H., Yaghi O. M., Highly Porous and Stable Metal-Organic Frameworks: Structure Design and Sorption Properties, *J. Am. Chem. Soc.* **122** (2000) pp. 1391-1397.
101. Eddaoudi M., Kim J., Rosi N., Vodak D., Wachter J., O'Keeffe M. and Yaghi O. M., Systematic Design of Pore Size and Functionality in Isoreticular MOFs and Their Application In Methane Storage, *Science* **295** (2002) pp. 469-472.
102. Chen B., Eddaoudi M., Reineke, T. M., Kampf, J. W., O'Keeffe M. and Yaghi O. M., $\text{Cu}_2(\text{ATC}) \cdot 6\text{H}_2\text{O}$: Design of Open Metal Sites in Porous Metal-Organic Crystals (ATC: 1,3,5,7-Admantane Tetracarboxylate), *J. Am. Chem. Soc.* **122** (2000) pp. 11559-11560.
103. Reineke T. M., Eddaoudi M., Fehr M., Kelley D. and Yaghi O. M., From Condensed Lanthanide Coordination Solids to Microporous Frameworks Having Accessible Metal Sites, *J. Am. Chem. Soc.* **121** (1999) pp. 1651-1657.

-
104. Seo J. S., Whang D., Lee H., Jun S. I., Oh J., Jeon Y. J. and Kim K. A homochiral metal-organic porous material for enantioselective separation and catalysis, *Nature* **404** (2000) pp. 982-986.
 105. Seki K., Design of an adsorbent with an ideal pore structure for methane adsorption using metal complexes., *Chem. Commun.* (2001) pp. 1496-1497.
 106. Noro S., Kitagawa S., Kondo M. and Seki K. A New Methane Adsorbent, Porous Coordination Polymer [$\{\text{CuSiF}_6(4,4'\text{-bipyridine})_2\}_n$], *Angew. Chem. Int. Ed.* **39** (2000) pp. 2082-2084.
 107. Yaghi O. M. and Li H., T-Shaped Molecular Building Units in the Porous Structure of $\text{Ag}(4,4'\text{-bpy})\cdot\text{NO}_3$, *J. Am. Chem. Soc.* **118** (1996) pp. 295-296.
 108. Yaghi O. M., Li H., Davis C., Richardson D. and Groy T., Synthetic Strategies, Structure Patterns, and Emerging Properties in the Chemistry of Modular Porous Solids, *Acc. Chem. Res.* **31**, pp. 474-484.
 109. Eddaoudi M., Moler D. B., Li, H., Chen B., Reineke T. M., O'Keeffe, M. and Yaghi O. M., Modular Chemistry: Secondary Building Units as a Basis for the Design of Highly Porous and Robust Metal-Organic Carboxylate Frameworks. *Acc. Chem. Res.* **34** (2001) pp. 319-330.
 110. Wang Q. M., Shen D., Bulow M., Lau M. L., Deng S. Fitch F. R., Lemcoff N. O. and Semanscin J., Metallo-organic molecular sieve for gas separation and purification, *Microporous Mesoporous Mater.* **55** (2002) pp. 217-230.
 111. Tao J., Tong M., Shi J., Chen X., Ng S. W., Blue photoluminescent zinc coordination polymers with supertetranuclear cores, *Chem. Commun.* (2000) pp. 2043-2044.
 112. Lin C. Z-J., Chui S. S-Y, Lo S. M-F., Shek F. L-Y, Wu M., Suwinska K., Lipkowski J. and Williams I. D., Physical stability vs. chemical stability in microporous metal coordination polymers: a comparison of $[\text{Cu}(\text{OH})(\text{INA})]_n$ and $[\text{Cu}(\text{INA})_2]_n$: INA = 1,4-($\text{NC}_3\text{H}_4\text{CO}_2$), *Chem. Commun.* (2002) pp. 1642-1643.
 113. Abrahams B. F., Hoskins B. F., Michail D. M. and Robson R., Assembly of porphyrin building blocks into network structures with large channels, *Nature* **369** (1994) pp. 727-729.
 114. Kosal M., Chou J., Wilson S. R., and Suslick K. S., A functional zeolite analogue assembled from metalloporphyrins, *Nature Mater.* **1** (2002) pp. 118-121.
 115. Lin K-J, SMTP-1: The First Functionalized Metalloporphyrin Molecular Sieves with Large Channels, *Angew. Chem. Int. Ed.* **38** (1999) pp. 2730-2732.
 116. Yang S. Y., Long L. S., Jiang Y. B., Huang R. B., Zheng L. S., An Exceptionally Stable Metal-Organic Framework Constructed from the $\text{Zn}_8(\text{SiO}_4)$ Core, *Chem. Mater.* **14** (2002) pp. 3229-3231.
 117. Kim J., Chen B., Reineke T. M., Li H., Eddaoudi M., Moler D. B., O'Keeffe M. and Yaghi O. M., Assembly of Metal-Organic Frameworks from Large

-
- Organic and Inorganic Secondary Building Units: New Examples and Simplifying Principles for Complex Structures, *J. Am. Chem. Soc.* **123** (2001) pp. 8239-8247.
118. Hagrman D., Hagrman P., and Zubieta J., Solid-State Coordination Chemistry: The Self-Assembly of Microporous Organic-Inorganic Hybrid Frameworks Constructed from Tetrapyrrolylporphyrin and Bimetallic Oxide Chains or Oxide Clusters, *Angew. Chem. Int. Ed.* **38** (1999) pp. 3165-3168.
 119. Zheng N., Bu X., Feng P., Self-Assembly of Novel Dye Molecules and $[\text{Cd}_8(\text{SPh})_{12}]^{4+}$ Cubic Clusters into Three-Dimensional Photoluminescent Superlattices, *J. Am. Chem. Soc.* **124** (2002) pp. 9688-9689.
 120. Davis M. E., The Quest for Extra-Large Pore, Crystalline Molecular Sieves, *Chem. Eur. J.* **3** (1997) pp. 1745-1750.
 121. Freyhardt C. C., Tsapatsis M., Lobo R. F., Balkus K. J. Jr. and Davis M. E., A high-silica zeolite with a 14-tetrahedral-atom pore opening, *Nature* **381** (1996) pp. 295-298.
 122. Lobo R. F., Tsapatsis M., Freyhardt C. C., Khodabandeh S., Wagner P., Chen C., Balkus K. J. Jr., Zones S. I. and Davis M. E., Characterization of the Extra-Large Pore Zeolite UTD-1, *J. Am. Chem. Soc.* **119** (1997) pp. 8474-8484.
 123. Wagner P., Yoshikawa M., Lovallo M., Tsuji K., Taspatsis M. and Davis M., CIT-5: a high-silica zeolite with 14-ring pores, *Chem. Commun.* (1997) pp. 2179-2180.
 124. Yoshikawa M., Wagner P., Lovallo M., Tsuji K., Takewaki T., Chen C., Beck L. W., Jones C., Tsapatsis M., Zones S. I. and Davis M. E., Synthesis, Characterization, and Structure Solution of CIT-5. A new, High-Silica, Extra-Large-Pore Molecular Sieve, *J. Phys. Chem. B* **102** (1998) pp. 7139-7147.
 125. Barrett P. A., Diaz-Cabanas M. J., Cambor M. A. and Jones R. H., Synthesis in fluoride and hydroxide media and structure of the extra-large pore pure silica zeolite CIT-5, *J. Chem. Soc., Faraday Trans.* **94** (1998) pp. 2475-2481.
 126. Moore P. B. and Shen J., An X-ray structural study of cacoxenite, a mineral phosphate, *Nature* **306** (1983) pp. 356-358.
 127. Estermann M., McCusker L. B., Baerlocher C., Merrouche A., Kessler H., A Synthetic Gallophosphate molecular sieve with a 20-tetrahedral-atom pore opening, *Nature* **352** (1991) pp. 320-323.
 128. Jones R. H., Thomas J. M., Chen J. Xu R., Huo Q., Li S., Ma Z. Chippindale A. M., Structure of an Unusual Aluminum Phosphate $[\text{Al}_5\text{P}_6\text{O}_{24}\text{H}]^{2-} \cdot 2[\text{N}(\text{C}_2\text{H}_5)_3\text{H}]^+ \cdot 2\text{H}_2\text{O}$ JDF-20 with large elliptical Apertures, *J. Solid State Chem.* **102** (1993) pp. 204-208.
 129. Richardson J. W. Jr. and Vogt E. T. C., Structural determination and Rietveld refinement of aluminophosphate molecular sieve $\text{AlPO}_4\text{-8}$, *Zeolites* **12** (1992) pp. 13-19.

-
130. Guillou N., Gao Q., Forster P. M., Chang J., Nogues M., Park S., Ferey G. and Cheetham A. K., Nickel(II) Phosphate VSB-5: A Magnetic Nanoporous Hydrogenation Catalyst with 24-ring Tunnels, *Angew. Chem. Int. Ed.* **40** (2001) pp. 2831-2834.
 131. Guillou N., Gao Q., Nogues M., Morris R. E., Hervieu M., Ferey G. and Cheetham A. K., Zeolitic and magnetic properties of a 24-membered ring porous nickel(II) phosphate, VSB-1, *C. R. Acad. Sci. Paris, t. 2, Serie II c* (1999) pp. 387-392.
 132. Brunner G. O., "Quantitative zeolite topology" can help to recognize erroneous structures and to plan syntheses, *Zeolites* **13** (1993) pp. 88-91.